Oxygen isotopes and volatile contents of the Gorgona komatiites, Colombia: a confirmation of the deep mantle origin of H_2O

Andrey A. Gurenko[1]*, Vadim S. Kamenetsky[2], Andrew C. Kerr[3]

[1] *Centre de Recherches Pétrographiques et Géochimiques, UMR 7358, Université de Lorraine, 54501 Vandoeuvre-lès-Nancy, France*

[2] *School of Physical Sciences, University of Tasmania, Private Bag 79, Hobart, TAS 7001, Australia*

[3] *School of Earth and Ocean Sciences, Cardiff University, Park Place, Cardiff, UK, CF10 3AT*

Revised manuscript

submitted to *Earth and Planetary Science Letters*

10 August, 2016

Components: abstract (333 words; 2,114 characters with spaces),

main text (8,258 words; 53,382 characters with spaces),

6 figures, 0 tables,

the list of references includes 102 citations.

* **Corresponding author and present address:** Andrey A. Gurenko, Centre de Recherches Pétrographiques et Géochimiques, 15, rue Notre-Dame des Pauvres, BP 20, 54501 Vandoeuvre-lès-Nancy, France. Phone: +33 (0)3 83 59 48 75, Fax: +33 (0)3 83 51 17 98, E-mail: agurenko@crpg.cnrs-nancy.fr

Abstract

We report O isotopes in olivine grains ($Fo_{89–93}$) and volatile contents (CO_2, H_2O, F, S, Cl) in olivine-hosted melt inclusions from one Gorgona picrite and five komatiites with the aim of constraining the origin of H_2O in these magmas. These samples have previously been analysed for major and trace elements and volatile concentrations (H_2O, S, Cl) and B isotopes in melt inclusions. A distinctive feature of the included melts is relatively high contents of volatile components and boron, which show positive anomalies in, otherwise depleted, primitive mantle normalised trace and rare earth element patterns and range in $\delta^{11}B$ from −11.5 to 15.6‰. In this study, the olivines were systematically analysed for O isotopes (1) in the centre of grains, (2) near the grain boundaries and, (3) as close as possible to the studied melt inclusions. The majority of olivines (~66%) are "mantle"-like, 4.8‰ ≤ $\delta^{18}O$ ≤ 5.5‰, with a subordinate but still significant number (~33%) above, and only 2 grains below, this range. There is no systematic difference between the central and marginal parts of the grains. Higher than "mantle" $\delta^{18}O_{Ol}$ values are ascribed to low-T (<300 ºC) serpentinisation along inner fractures and grain boundaries of olivine phenocrysts. The measured concentrations of volatile components in the melt inclusions corrected for the effects of post-entrapment crystallisation and H_2O-CO_2 exsolution in inclusion shrinkage bubbles are: 286–1748 µg/g CO_2, 0.2–0.86 wt.% H_2O, 48–82 µg/g F, 398–699 µg/g S and 132–198 µg/g Cl. They correspond to a pressure of 86 ± 44 MPa or ~2.5-km crustal depth of olivine crystallisation. The correlations of S and, to a lesser extent, of H_2O, with highly incompatible lithophile elements and the correlation of F with Cl, but no relationships of H_2O with Cl, rule out shallow depth magma degassing and/or crustal contamination. Our new $\delta^{18}O$ olivine and volatile component data combined with the existing, highly variable $\delta^{11}B$ values for melt inclusions also support the deep mantle origin of H_2O (and probably other volatiles) in the Gorgona mafic and ultramafic magmas.

Keywords

Gorgona Island, Komatiites, Olivine, Oxygen isotopes, Volatile components, Ion microprobe

1. Introduction

Komatiites are olivine spinifex-textured, ultramafic, mantle-derived rocks formed by high degrees of partial melting and typically having high magnesium (>18 wt.% MgO), with low silicon (40–45 wt.% SiO_2), titanium (<1 wt.% TiO_2) and incompatible trace element concentrations (e.g., Arndt and Nisbet, 1982; Kerr and Arndt, 2001 and references therein). Komatiites were first recognized in the late 1960s in the Barberton greenstone belt, South Africa, and were named from their type locality along the Komati River (Viljoen and Viljoen, 1969a,b). There has long been a considerable debate as to whether komatiites are derived from dry and hot mantle, and are the products of partial melting of ascending super-hot Archaean plumes (e.g., Bickle et al., 1977; Campbell et al., 1989; McDonough and Ireland; 1993; Arndt et al., 1997, 1998; Herzberg et al., 1995, 2007; Berry et al., 2008 among others) or are formed by hydrous melting of the mantle at much lower temperatures during subduction (e.g., Allègre, 1982; Parman et al., 1997; Grove and Parman, 2004; Parman and Grove, 2005). Because most komatiites have undergone significant sub-solidus alteration, primary volatile abundances of the magmas from which they crystallised, remain controversial.

In this context, the Late Cretaceous (~90 Ma) ultramafic and mafic lavas of the Gorgona Island, Colombia, first identified as komatiites by Gansser et al. (1979) and then studied in more detail by e.g., Echeverría (1980), Dietrich et al. (1981), Aitken and Echeverría (1984), Echeverría and Aitken (1986), Kyser et al. (1987), Kerr et al. (1996), Arndt et al (1997), Kerr (2005), Révillon et al. (2000, 2002), Serrano et al. (2011), among others, represent suitable candidates for the study of volatile components because they are generally much fresher compared to most of their Archaean counterparts. In addition, the komatiites from Gorgona remain the only known non-Archaean komatiites and, therefore, studying them in detail may have important implications for our understanding the effects of water on mantle potential temperatures.

Although, overall, olivine-hosted melt inclusions in Gorgona komatiites are depleted in incompatible trace elements, they are distinctive in that they possess relatively high concentrations of volatile components and boron (Kamenetsky et al., 2010). These high concentrations result in positive anomalies (10 to 50 fold enrichment) on primitive mantle normalised trace and rare earth element diagrams and a wide range of δ^{11}B values from −11.5 to +15.6‰. Based on these data, Gurenko and Kamenetsky (2011) concluded that the inclusions with "mantle"-like δ^{11}B (around −10‰), also enriched in H_2O and Cl, represent the unmodified composition of their parental magmas. Moreover, they demonstrated that although a range of contaminants (seawater, NaCl saline brines, altered oceanic crust, serpentinised peridotite or marine sediments) could potentially affect the composition of these magmas, the observed volatile enrichment could be better explained by possible input of less than 3 wt.% of a H_2O- and ^{11}B-enriched fluid into the source of the Gorgona komatiites.

The present work is follow-up study (from the work of Kamenetsky et al., 2010); Gurenko and Kamenetsky, 2011) on olivines from Gorgona komatiites and their included melts and primarily focuses on their detailed oxygen isotopic composition, determined by SIMS (= Secondary Ion Mass Spectrometry). The main purpose of the present study is therefore to further constrain the origin of volatile components, and especially H_2O in the Gorgona parental magmas. Furthermore, in order to evaluate the pressure (or depth) of olivine crystallization (with the aim of discriminating between upper and lower crust levels, which presumably have different O-isotope signatures), and to place additional constraints on the behaviour of volatile components during magma origin and consequent crystallization, we re-analysed the same olivine-hosted melt inclusions remaining after the Kamenetsky et al. (2010) and Gurenko and Kamenetsky (2011) SIMS and laser ablation ICP-MS measurements. These previously studied melt inclusions, together with several newly exposed inclusions were analysed for CO_2, H_2O, F, S and Cl (note that neither CO_2 nor F concentrations were previously reported). Based on the existing

and our new volatile component and O-isotope data, this study will help to determine if the ascending high-Mg melts, currently preserved as inclusions in olivine, have suffered contamination by either crustal rocks at shallow depth (Arndt et al., 1997), or by seawater or seawater-derived components (Shimizu et al., 2009). If such contamination has occurred, one would expect a deviation of $\delta^{18}O$ measured in the studied Gorgona olivines from that of the mantle (4.8–5.8‰; Mattey et al., 1994; Eiler, 2001) to more ^{18}O-enriched values. In this context, our new oxygen isotope data on olivines, when coupled with the available volatile contents and boron isotope data on melt inclusions will be key to unravelling the origin of wet high-Mg magmas, now preserved as komatiites and picrites on the island of Gorgona.

2. Geological setting and samples

Gorgona is located ~40 km off the Pacific coast of Colombia (**Fig. 1**). The geology of this small island (approximately 8.3 km long and 2.5 km wide), was first studied by Gansser (1950), who noted the occurrence of "olivine rocks" containing skeletal olivine phenocrysts, which later were recognised as "komatiites" by Gansser et al (1979) and Echeverría (1980). Echeverría (1980) also reported picrites from the south part of the island that had no skeletal olivine crystals. An undeformed peridotite-gabbro complex is located in the central part of the island and surrounded by a sequence of tilted and faulted blocks of mafic and ultramafic rocks and tuff breccias (Dietrich et al., 1981; Aitken and Echeverría, 1984). The first petrographic and geochemical work on these rocks was reported by Dietrich et al. (1981) and Echeverría (1980) and demonstrated that the olivine spinifex (komatiite) lavas contain 13 to 24 wt.% MgO. Aitken and Echeverría (1984) proposed that the parental magma of the komatiites contained ~20 wt.% MgO. Kyser et al. (1987) reported the first stable isotope (δD and $\delta^{18}O$) data on Gorgona komatiites.

Our present work is based on the same 50 olivine fragments studied by Kamenetsky et al. (2010) and Gurenko and Kamenetsky (2011). These fragments contain small portions of melt entrapped along zones of skeletal growth of the former euhedral to subhedral olivine phenocrysts, as well as 21 additional, randomly selected olivine phenocrysts from a picrite sample GOR94-32. The komatiitic samples were collected from fresh coastal exposures on the north east side of the island (**Fig. 1**; for more detail, see Kamenetsky et al., 2010).

Sample GOR94-32 was collected from a picrite lava block, whose whole rock geochemistry was reported by Arndt et al. (1997). As first noted by Echeverría and Aitken (1986) and studied subsequently by Kerr et al. (1996), Révillon et al. (2000) and Kerr (2005), the fragmental picritic rocks (with angular-to-rounded blocks ranging in size from a few centimetres to > 1 m) and picritic tuffs are exposed in the southern part of the island and are intruded by a suite of comagmatic dykes (**Fig. 1**). As noted by Kerr (2005), the picrite blocks comprise ~25 vol.% euhedral, non-skeletal olivine phenocrysts (0.5–1.0 mm), set in a groundmass of very fine-grained Cr-spinel microphenocrysts and acicular crystals of clinopyroxene and plagioclase.

3. Analytical methods

Oxygen isotopic composition of olivine grains was systematically analysed by ion microprobe. Several previously studied and newly exposed olivine hosted melt inclusions were also analysed for CO_2, H_2O, F, S and Cl concentrations by SIMS. In order to check that no host olivine was ablated by the ion beam, the spot position was carefully examined with a petrographical microscope after analysis. As an additional check, aluminium (since it is incompatible in olivine but present in the melt inclusions in concentrations >15 wt.% Al_2O_3) was also included in the analytical sequence along with the volatile components in order to monitor and correct for any ablation of olivine (for more detail, see *Supporting online material*). Following these analyses, olivine composition was re-analysed by electron microprobe (hereafter

156 EPMA = Electron Probe Microanalysis) as close as possible (10–30 μm) to the spots left by
157 SIMS. Most of the studied olivines were analysed for major elements by Kamenetsky et al.
158 (2010). However, here we report and discuss only the newly acquired olivine major element
159 data, except for four olivine grains that were lost during remounting from an epoxy mount into
160 indium metal. For these olivines, we use major element compositions published in Kamenetsky
161 et al. (2010).
162
163 **4. Results**
164 *4.1. Elemental and oxygen isotope variability of olivines*
165 The olivines were systematically analysed for oxygen isotopes: a) in the centre of grain,
166 b) near the grain boundaries and c) as close as possible to the previously studied and newly
167 exposed melt inclusions. As noted by Kamenetsky et al. (2010), olivine phenocrysts from the
168 studied komatiite samples are serpentinised along inner fractures and grain margins.
169 Consequently only smaller fragments of former olivine phenocrysts remained intact for
170 geochemical analysis and the melt inclusion study. For this reason, no direct link exists between
171 internal and external parts of the analysed grains and the true cores and rims of the former
172 olivine crystals.
173 The analyses of oxygen isotopes were replicated 2 to 28 times (except for 2 of 71 olivine
174 grains that were analysed only in one spot) during three separate analytical sessions (for
175 reproducibility results, see **Fig. S1.1** of *Supporting online material*). In total, 138 oxygen isotope
176 analyses of olivine, each based on an average of up to 14 spot analyses (in total 824 individual
177 $^{18}O/^{16}O$ determinations) were completed during the present study.
178 The olivines from the Gorgona picrite sample (GOR94-32) have a wider range of
179 forsterite contents that extend to higher values ($Fo_{88.3–93.2}$), as compared to those from the
180 komatiite samples ($Fo_{88.3–91.5}$), and contain 0.29–0.38 wt.% CaO, 0.34–0.46 wt.% NiO,

0.09–0.19 wt.% Al_2O_3 and 0.07–0.17 wt.% Cr_2O_3). However, the olivines from this picrite have systematically lower NiO concentrations than the komatiite olivines at equivalent Fo contents, resulting in two distinct trends of olivine crystallisation (**Fig. 2a, b**). These trends are in agreement with the observation of Kerr et al. (1996), who noted that Gorgona picrites usually have lower Fe_2O_3, Ni and Zr and somewhat higher Sc and Y concentrations (at a given MgO) than the komatiites. We think that the observed narrow Fo-ranges within individual samples (ΔFo = Fo_{max} – Fo_{min} for a given sample is between 0.6 and 3.2 mol.% in komatiites and 4.9 mol.% in picrite; **Fig. 2a**), similar concentrations of NiO (0.36–0.50 wt.%, except for one grain with 0.32 wt.%; **Fig. 2b**), CaO (0.3–0.36 wt.%, except for one grain with 0.4 wt.%), Al_2O_3 (0.07–0.14 wt.%) and Cr_2O_3 (0.07–0.15 wt.%) **(Table S2.1** – *Supporting online material*), and almost complete overlap of the compositions of the internal and external parts of the studied olivine fragments imply almost no elemental intra-crystal zoning.

The $\delta^{18}O_{Ol}$ span a range of values between 4.7 and 6.0‰ **(Fig. 2c, d)**. Because most individual grains were multiply analysed in the centre of the grain and near the grain boundaries, the average external precision of $\delta^{18}O_{Ol}$ determinations in the internal and external grain zones is ±0.2‰, 2 SE (broad range is 0.07–0.47‰). The majority of $\delta^{18}O_{Ol}$ values (~66% i.e., 91 of 138) are mantle-like, with $\delta^{18}O_{Ol}$ ranging from 4.8 to 5.4‰. A significant number of $\delta^{18}O_{Ol}$ determinations (~33%, i.e., 45 of 138) exceed the "mantle" range towards higher values, and only two of 138 are below 4.8‰. The probability density distribution curves calculated using *Isoplot 3.70* (Ludwig, 2008) reveal a common maximum of $\delta^{18}O_{Ol}$ at ~5.3‰ for most of the studied olivine "cores" and "rims" **(Fig. 2e)**, but the "rims" exhibit also an additional, subordinate peak at ~5.6‰. The absence of systematic differences (or zoning) in both Fo and $\delta^{18}O_{Ol}$ values between internal and external parts of the grains can be interpreted as evidence for only minor interaction of the crystallised olivines with a second primitive or evolved magma, or interaction of the olivine parental magma with surrounding crustal rocks.

Prior to this study only a limited amount of oxygen isotope data was available for Gorgona mafic rocks: Kyser et al. (1987) reported (from two basalts and one picrite) a range of $\delta^{18}O$ from 6.0 to 6.3‰ for olivine and 7‰ for one clinopyroxene. The results of this study were interpreted as supporting a mantle origin of the Gorgona komatiites, suggesting that the mantle source of these rocks may have been more fertile, compared to that of Archaean komatiites. Moreover, the δD and $\delta^{18}O$ values obtained for chrysolite from Gorgona komatiitic samples by Kyser et al. (1987) were interpreted to be consistent with serpentinisation by meteoric water rather than from seawater. A subsequent study by Révillon et al. (2002) reported a $\delta^{18}O$ range from 5.25 to 5.73‰ for clinopyroxene separates from the Gorgona picrites and komatiites. Accordingly, using the oxygen isotope fractionation factor between olivine and clinopyroxene ($\Delta^{18}O_{Cpx-Ol}$ = 0.33–0.37; Chiba et al., 1989), the $\delta^{18}O_{Ol}$ equivalent calculated for 1300–1400ºC using the above clinopyroxene O-isotope data is in the range of 4.9–5.4‰, i.e., values that are similar to the O-isotope range obtained in the present study.

4.2. Volatile concentrations

As previously shown by Kamenetsky et al. (2010) and Gurenko and Kamenetsky (2011), melt inclusions from the studied Gorgona olivines are characterised by pronounced enrichment of volatile components (0.2–1.0 wt.% H_2O, 520–770 µg/g S, 220–310 µg/g Cl) and boron (0.61–2.02 µg/g B) which show positive anomalies in, otherwise depleted, primitive mantle normalised trace element and REE patterns. In order to constrain a minimum pressure (or depth) of olivine crystallisation (with the aim of discrimination between upper and lower crustal rocks that have different O-isotope composition; e.g., Gregory and Taylor, 1981), and to place additional constraints on the behaviour of volatile components during magma origin and consequent crystallization, we re-analysed 6 melt inclusions remaining after SIMS and laser ablation ICP-MS measurements, whose compositions are reported in Kamenetsky et al. (2010)

and Gurenko and Kamenetsky (2011), and analysed 9 additional melt inclusions for CO_2, H_2O, F, S and Cl by SIMS. More detailed information about the selection and preparation of melt inclusions prior to analysis, and their laboratory heating and quenching conditions is given in Kamenetsky et al. (2010). No melt inclusions in olivine from the picrite sample GOR94-32 were analysed during the present study.

Prior to interpreting the existing volatile data it is important to assess whether the original concentrations of water dissolved in the included melts are compromised by possible diffusive gain or loss of H_2O through olivine host. Such diffusion of H_2O was first noted by Sobolev and Danyushevsky (1994) and then experimentally investigated by Portnyagin et al. (2008) and other more recent studies. The problem of possible rapid exchange of water between melt inclusions in olivine and a host magma in relation to the studied Gorgona melt inclusions were briefly discussed in Kamenetsky et al. (2010), who have concluded that "…the enrichment of the studied melt inclusions in the volatile elements is magmatic in origin" (page 1005). Moreover, if H_2O was acquired by the inclusions due to H^+-diffusion inside olivine hosts, this would imply the existence of a H_2O-rich ambient magma, from which the olivines with "normal mantle" $\delta^{18}O$ signature have crystallized. The existence of such a H_2O-rich magma would additionally support our previous conclusion about wet origin of the Gorgona komatiites. We thus maintain that the only process that could potentially bias water concentrations is H_2O-loss that could also happen during laboratory heating of the inclusions. However, several lines of evidence argue against extensive loss of H_2O during olivine crystallisation at depth or upon eruption:

1. The first and compelling evidence arguing against possible diffusive gain or loss of H_2O is existence of multiple significant correlations between volatile components, especially H_2O, and major (SiO_2 in the case of H_2O) and multiple incompatible trace elements (see below).

We contend that if the concentrations of water in the melt inclusions have been compromised, it is unlikely that these correlations would be preserved.

2. A main signature of the Gorgona komatiites is a spinifex texture that points towards the exceptionally fast crystallization of the parental magma resulting in formation of skeletal olivine. These olivine crystals contain very few melt inclusions and a search of >20,000 olivine fragments provided us with only a few tens of inclusions from ~ 30 μm to ~60 μm size used in this and our previous studies (see respective phototables in Kamenetsky et al., 2010 and Gurenko and Kamenetsky, 2011). We contend that the studied fragments of skeletal olivine containing melt inclusions formed during and shortly after emplacement of the parental magma as a result of its rapid cooling, suggesting that there was virtually no time to compromise H_2O concentrations in the included melts. Moreover, the observed wide variations in H_2O in the studied melt inclusions (0.3–1.1 wt.%; see below), in contrast to relatively narrow variations in forsterite content of the olivine hosts (Fo 90.7 ± 0.6 mol.%, excluding more evolved GOR94-17 komatiite and GOR94-32 picrite samples) would additionally support the absence of post-entrapment H_2O re-equilibration, otherwise no H_2O-range would have been preserved in the inclusions.

3. Formation of a spinifex texture requires not only rapid cooling of MgO-rich parental magma but also the cooling must occur in a strong thermal gradient (7–35 ºC/cm; Faure et al., 2006). If the parental magma ponded in a magma reservoir and had begun to crystallise olivine, the thermal gradient is unlikely to have been strong enough, and the cooling too slow, to form spinifex-textured olivine. All this argues against extensive olivine fractionation in a plumbing system, where diffusive H_2O loss might occur. However unlike komatiites, the studied picrite GOR94-32 is characterized by compositionally diverse olivine phenocrysts (Fo 91.4 ± 1.2 mol.%), which show no skeletal appearance and contain abundant partially crystallised, glassy

inclusions. It is therefore possible that in contrast to komatiites, H_2O contents in melt inclusions from this picrite sample could be strongly compromised.

4. An additional argument in support of the rapid quenching of komatiite parental magma could be the presence of clusters of Cr-spinel crystals in the groundmass of the studied rocks. Many of these spinel crystals, although extending to more Fe-rich compositions, are compositionally similar to those included in olivine and exhibit no rims enriched in both ulvöspinel and magnetite components (in contrast to what could be observed, if a host magma had a long crystallization history; e.g., Kamenetsky et al., 2001; Gurenko et al., 2006). Given that the majority of olivine-hosted spinel inclusions are in the same growth zones of skeletal olivine (as the melt inclusions), this suggests rapid crystallization of spinel occurred in the rising and erupted magma along with its nearly simultaneous entrapment by growing olivine.
5. Partial loss of H_2O from inclusions during laboratory heating is possible and thus the concentrations of H_2O in the included melts have to be considered as lower-end estimates. However as noted by Sobolev et al (2016) in Archaean komatiites, melt inclusions with a diameter >30 μm appear to preserve unbiased H_2O concentrations if magma was cooling fast (while forming spinifex), as well as during laboratory heating. Moreover, the existing significant correlations of H_2O with incompatible elements (see below) suggest that this process is unlikely to have had a significant effect.

The present results of volatile analysis in the studied melt inclusions are listed in **Table S2.2** (*Supporting online material*), along with the volatile concentrations, boron contents and isotopic composition obtained by Kamenetsky et al. (2010) and Gurenko and Kamenetsky (2011). The following observations can be made based on these data:

1. The concentrations of volatile components in the analysed melt inclusions (35–297 µg/g CO_2, 0.26–1.11 wt.% H_2O, 67–107 µg/g F, 556–879 µg/g S and 186–304 µg/g Cl) are in very good agreement with our previously published data set. Correction for post entrapment crystallization of olivine (14–38 wt.% Ol; **Table S2.2 –** *Supporting online material*) results in the following ranges: 26–222 µg/g CO_2, 0.2–0.83 wt.% H_2O, 52–86 µg/g F, 431–730 µg/g S and 142–209 µg/g Cl. Comparison of these ranges with those reported for chromite-hosted melt inclusions by Shimizu et al. (2009) (up to 4000 µg/g CO_2 and below 0.4 wt.% H_2O, except for one inclusion with 0.91 wt.% H_2O), reveals that almost all inclusions analysed in the present study are characterised by significantly lower CO_2 concentrations but have higher H_2O at an equivalent CO_2 (**Fig. 3a)**.
2. Decompression degassing of magma results in preferential exsolution of CO_2 (as opposed to H_2O) into vapour phase (Dixon and Stolper, 1995). The concentrations of H_2O and CO_2 directly measured by SIMS in the Gorgona melt inclusions reflect the last vapour-melt equilibrium in the magmatic system for the time of eruption and thus represent a minimum pressure of magma fractionation, as the melts could have been partially degassed. According to the *VolatileCalc* solution model (Newman and Lowenstern, 2002), they correspond to H_2O-CO_2 gas pressures between 5 and 30 MPa or to <1-km crustal depth (**Fig. 3a**).
3. Numerous studies (Esposito et al., 2011; Steele-Macinnis et al., 2011; Hartley et al., 2014; Moore et al., 2015; Wallace et al., 2015; Mironov et al., 2015) have demonstrated that 40 to 90% of the original CO_2 dissolved in the melt at the time of inclusion entrapment can be lost to a shrinkage bubble during post-entrapment cooling. A correction algorithm described by Wallace et al. (2015) was therefore used to reconstruct the original CO_2 and H_2O concentrations in the included melts (see *Supporting online material*). These calculations reveal that 79–92% (average 87%) of the original CO_2 and 1–5% (average 2%) of the original H_2O have been lost to the shrinkage bubble, in agreement with the results of the above

studies. The following ranges of volatile concentrations were obtained after correction: 286–1748 µg/g CO_2, 0.2–0.86 wt.% H_2O, 48–82 µg/g F, 398–699 µg/g S and 132–198 µg/g Cl. According to the *VolatileCalc* solution model (Newman and Lowenstern, 2002), these results correspond to H_2O-CO_2 gas pressures between 20 and 200 MPa (average 86 ± 44 MPa, 1 SD; **Table S2.2 –** *Supporting online material*) or to ~2.5-km crustal depth **(Fig. 3b)**.

4. The concentrations of sulphur (either corrected for post entrapment crystallisation and shrinkage bubble volatile exsolution or not) are lower than those of MORB and ocean island basalt (OIB) submarine glasses (usually S >800 µg/g at ~7–10 wt.% FeO; Wallace and Carmichael, 1992), but plot above the "sulphur saturation line" defined by compositions of sulphide saturated experimental melts from Haughton et al. (1974) (**Fig. 4a**). The presence of micron-scale sulphide globules inside several melt inclusions suggests saturation of the included melts with sulphur. It is possible that this saturation might be caused by post-entrapment loss of Fe from the inclusions (Danyushevsky et al., 2002). However, there is good positive correlation of S with Ce (R^2 = 0.77 and 0.96 for uncorrected and corrected S concentrations, respectively, except for one outlier; **Fig. 4b**), as well as significant correlations of S with other incompatible elements [e.g., Ti (0.87), Sr (0.71), Zr (0.61), Ba (0.47), La (0.54), Pr (0.67), Nd (0.49), Sm (0.42), Eu (0.64), Tb (0.77), Ho (0.58), Er (0.81), Lu (0.56), Hf (0.53); the respective R^2 values for corrected S concentrations are given in brackets]. Such relationships cannot be explained by either the later, post-entrapment origin of sulphide phase in the inclusions or by magma contamination, but may imply incompatible behaviour of S at an early stage of magma fractionation and probably undersaturation of high-Mg "primary" magma with sulphur, as demonstrated on MORB magmas by Sobolev and Hofmann (1999).

5. Similarly, H_2O concentrations (in particular, post-entrapment crystallisation- and shrinkage bubble-corrected values) have a clear positive correlation with SiO_2 (R^2 = 0.60) **(Fig. 4c)** and

still significant negative correlations with some incompatible elements, such as Ti (0.50), Sr (0.43), Y (0.43), Zr (0.54), Ce (0.44), Sm (0.79), Dy (0.49), Ho (0.73), Er (0.58), Tm (0.43), Yb (0.74), Lu (0.46); the respective R^2 values are given in brackets **(Fig. 4d)**.

6. There are, however, no correlations of H_2O with fluid mobile incompatible elements (e.g., Ba, K), Pb and Th, also implying that H_2O, along with S, might have not been degassed during magma fractionation at shallow depth. One possible explanation of the observed positive correlation of H_2O with SiO_2 (**Fig. 4c**) could be incompatible behaviour of water during magma fractionation. However, one would expect also a coherent increase in H_2O with increasing concentrations of the other incompatible elements. As this is not the case, we suggest that the correlation between SiO_2 and H_2O, in conjunction with negative trace element-H_2O correlations, could be explained by a gradual increase in the degree of partial melting of a clinopyroxene-depleted mantle source under hydrous conditions (e.g., Parman and Grove, 2004). The coherent increase in SiO_2 and H_2O contents in the magma can be explained by H_2O-fluxed decompression melting of refractory mantle accompanied by increasing contribution of orthopyroxene to the melting reaction, and consequent progressive depletion of trace element concentrations in the resulting melts.

7. The concentrations of chlorine in the included melts show no relationship with H_2O, CO_2 or S (as well as the ratios of these volatile component concentrations to those of incompatible elements, such as CO_2/Nb, H_2O/Ce, F/Zr, Cl/Nb, and S/Ce) but show a significant linear correlation with fluorine (R^2 = 0.43 and 0.46 for uncorrected and corrected concentrations, respectively) (**Fig. 4e**). Chlorine and fluorine usually behave as incompatible elements during partial melting and magma fractionation, if their juvenile concentrations were not affected by later degassing or contamination events (e.g., Carroll and Webster, 1994; Jambon, 1994). The observed F-Cl correlation may thus suggest that the reported F and Cl concentrations were not

influenced by degassing or contamination at crustal depth and are likely to reflect mantle derived compositions, in agreement with incompatible behaviour of S and H_2O.

5. Discussion

5.1. Message from oxygen isotopes

Oxygen isotopes represent one of the most effective ways of tracing crustal components in the source of mafic magmas and can provide robust constraints on shallow-level crustal contamination because fractionation of oxygen isotopes is much more significant in low-temperature hydrothermal processes, than in the mantle (e.g. Kyser et al., 1987; Woodhead et al., 1993; Eiler et al. 1995, 1996, 1997; Garcia et al., 1998; Harris et al., 2000, 2015; Widom and Farquhar 2003; Bindeman et al. 2005, 2006, 2008; Wang and Eiler, 2008; Day et al., 2009; Martin et al., 2011; Genske et al., 2013). Oxygen isotope heterogeneity of the oceanic crust is generally caused by seawater and/or seawater-derived fluid alteration (e.g., Muehlenbachs et al., 1974; Hattori and Muehlenbachs, 1982; Condomines et al., 1983; Muehlenbachs 1986; Alt et al., 1986). The oceanic crust can be affected by both low (<300–400°C) and relatively high (>400°C) temperature fluid-rock interaction. It can vary in oxygen isotopic composition with depth, mostly due to cross-over of oxygen isotopic fractionation factors (and their magnitude) between minerals and water at ~300°C. Indeed, most of the oceanic crustal rocks altered by seawater cover a ~10‰ range of $\delta^{18}O$ (from ~2–3‰ to ~11–13‰) spanning the "normal"-$\delta^{18}O$ mid-ocean ridge basalt (MORB) magma value of ~5.6 ± 0.2‰ (Gregory and Taylor, 1981; Alt et al., 1986; Stakes and Taylor, 1992; Bindeman, 2008; Martin et al., 2011; Yamaoka et al., 2012; Jacques et al., 2013 among others). But it is also never altered to $\delta^{18}O$ values lower than ~2‰ in its middle and lower sections because $\Delta^{18}O_{rock\text{-}water}$ isotope fractionation is effectively 0 ± 1‰ at high (>400°C) temperatures (Gregory and Taylor 1981; Stakes and Taylor 1992; Bindeman, 2008; Martin et al., 2011). During subsequent subduction and recycling, the relative proportions

of ^{18}O-enriched and ^{18}O-depleted material has been shown to remain broadly similar to those in the ocean crust prior to subduction, leading to δ^{18}O values in erupted volcanic-arc products that are distinct from that of pristine mantle (e.g., Bebout and Barton 1989; Putlitz et al. 2000).

Previous studies of tholeiitic to alkali basalts from Iceland, Hawaii, the islands of Tristan da Cunha, Gough, Canary and Azores (e.g., Harris et al., 2000; Bindeman et al., 2008; Wang and Eiler, 2008; Day et al., 2009; Genske et al., 2013) have demonstrated that a coherent decrease of $\delta^{18}O_{Ol}$ and Fo is most likely to be a signature of assimilation of low-δ^{18}O crustal rocks by ascending magma. This results in crystallization of olivine with lower than typical "mantle" (i.e., 4.8–5.4‰) δ^{18}O values from hybrid magma. The slope of such Fo-δ^{18}O relationships may vary significantly depending on the particular O-isotope composition of a contaminant, ranging from the most extreme case of Hawaii ($\delta^{18}O_{Ol}$ decreases from 5.3‰ to 4.6‰ in the range from Fo_{90} to Fo_{88} i.e., 0.35‰/mol.% Fo; Wang and Eiler 2008) through the Canaries (from 5.0‰ to 4.7‰ in the range from Fo_{84} to Fo_{79}, i.e. 0.06‰/mol.% Fo; Day et al., 2009) to the Azores ($\delta^{18}O_{Ol}$ = 5.2–4.8‰ in olivines $Fo_{90–77}$, i.e., 0.03‰/mol.% Fo) (see *contamination trends* in **Fig. 2c**). Conversely, olivine phenocrysts crystallized from mantle-derived magmas can show no clear signs of shallow-depth crustal contamination (for example, Society, Samoa and Canary islands, and the Karoo and Etendeka large igneous provinces). These olivine phenocrysts are characterised by elevated δ^{18}O relative to typical upper mantle values and this was ascribed to the presence of an ^{18}O-enriched component in the magma source (e.g., Eiler et al., 1997; Gurenko et al., 2011; Harris et al., 2015).

To justify such trends, the analytical precision of a "single grain" O-isotope determination must be at ±0.1–0.2‰, 2 SD, and such values are typical for laser fluorination analyses (e.g., Bindeman, 2008). In the case of SIMS measurements, one viable way to maintain the required analytical precision is to increase a number of individual measurements within a single grain. As noted above, most of the studied Gorgona olivine grains were multiply analysed

by SIMS. No substantial compositional difference has been recognised between internal and external parts of the grains, except for the second subordinate maximum in the "rim" probability density distribution curve at ~5.6‰ (**Fig. 2e**). As most of the studied olivine phenocrysts exhibit varying degrees of serpentinisation but no clear relationship of Fo with $\delta^{18}O_{Ol}$ **(Fig. 2c)**, and since shallow crustal contamination of the studied samples was not previously identified by Gurenko and Kamenetsky (2011) nor by our present volatile data, our preferred explanation for the second maximum and probably for the all $\delta^{18}O_{Ol}$ values in excess of the "mantle" range is a diffusive oxygen isotope exchange between olivine (4.8–5.4‰) and products of its low-temperature alteration (for example, with serpentine with $\delta^{18}O$ up to ~13‰; Martin et al., 2011).

A less probable possibility is that the shift to more positive $\delta^{18}O$ olivine compositions (**Fig. 2e**) could be related to admixture of a portion of a second magma derived from an ^{18}O-enriched mantle component, or by analogy with Martin et al. (2011) who reported $\delta^{18}O$ values of up to 6.1‰ in Mt. Shasta olivine phenocrysts, and related them to "a ^{18}O pre-enriched" peridotite mantle wedge component. However, we consider this explanation unlikely mostly because (a) the rapid, *in-situ* crystallisation (advocated herein) of skeletal olivine in the magma either en route to the surface or later in the lava flow would result in more diffused distribution of $\delta^{18}O_{Ol}$ values, with no well shaped maximums, as shown in **Fig. 2e**, and (b) the observed $\delta^{18}O$ enrichment is related to the edges of the studied olivine grains, which were in direct contact with serpentine filling grain fractures and whose origin can be ascribed to later alteration stage of the lava flows. In addition, a subordinate number of $\delta^{18}O$-enriched compositions determined for olivine "cores" (**Fig. 2e**) are ascribed to the so-called "3D-effect", when ion beam visually placed in the centre of a grain is in fact analysing its remaining outer part oriented parallel to the sample surface.

Calculation the average "single grain" $\delta^{18}O_{Ol}$ composition from all individual $\delta^{18}O_{Ol}$ measurements performed for each olivine grain, regardless of whether they represented "core" or

452 "rim" areas, results in the average standard deviation of mean external reproducibility of
453 ±0.12‰, 2 SE (grain to grain range from ±0.06 to ±0.26‰ due to the different number of
454 replicates), being comparable with those of single-grain laser fluorination. Figure 5 shows
455 averaged "within-grain" oxygen isotope compositions of the studied Gorgona olivines with no
456 discrimination between their internal and external zones. Like in **Fig. 2c**, no relationship between
457 Fo contents and $\delta^{18}O_{Ol}$ values for olivines can be observed for komatiite lavas. In contrast,
458 olivines from picrite GOR94-32 show a subtle positive correlation (R = 0.53), best approximated
459 by a polynomial quadratic equation **(Fig. 5a)**, which is significant at 95% confidence level
460 (critical value of the Pearson correlation coefficient R is 0.44 at N = 20). Similarly, as in **Fig. 2e**,
461 the probability density distribution curves reveal a common maximum of typical mantle $\delta^{18}O_{Ol}$
462 values between 5.2 and 5.3‰ **(Fig. 5b)**. A subordinate peak at ~5.6‰ for olivines from
463 komatiites and three less-pronounced subordinate peaks at ~5.6–5.9‰ for olivines from picrite
464 are thought to have been inherited from the analyses of rims.

465 If our assumption about the possible impact of later serpentinisation on the O-isotope
466 composition of olivine is correct, then some of the $\delta^{18}O_{Ol}$ values, including those from the
467 "mantle" range, could have been systematically shifted to more ^{18}O-enriched compositions. This
468 would result in more diffused shape of the maximums in the density distribution (**Fig. 2e**) and
469 representing the upper level of $\delta^{18}O_{Ol}$ estimates. Moreover, the absence of a clear relationship
470 between Fo content and $\delta^{18}O_{Ol}$ in komatiites also could be explained by this olivine-serpentine
471 O-isotope exchange, during which the isotopic composition of olivine was modified to a greater
472 extent than the Fo content (as serpentinisation does not affect forsterite number in olivine, as
473 recently shown by Birner et al., 2016). In this context, the most Fo-rich olivines of the "picrite"
474 trend in **Fig. 5a** having $\delta^{18}O_{Ol}$ values outside "mantle" range could be affected by this
475 serpentinisation process, suggesting also that their former unmodified $\delta^{18}O_{Ol}$ values originally
476 corresponded to the "normal" mantle $\delta^{18}O_{Ol}$ range.

477

478 *5.2. Evidence against crustal contamination*

479 The parental magmas of komatiites are hotter, up to 1600ºC for Archaean komatiites
480 (e.g., Herzberg et al., 2007 and references therein), as compared to MORB and OIB magmas,
481 and therefore are more likley to melt and assimilate surrounding wall rocks en route to the
482 surface. A melt inclusion study of 2.7-Ga-old Belingwe komatiites, Zimbabwe, demonstrated
483 that their parental magmas probably contained up to 1 wt.% H_2O, but the source of water was
484 uncertain (i.e., shallow magma contamination versus melting of a hydrous mantle plume source;
485 e.g., Shimizu et al., 2001; Berry et al., 2008; Kent et al., 2009). Recently, Sobolev et al. (2016)
486 reported marked H_2O enrichment of Archaean komatiites from the Abitibi greenstone belt,
487 Canada, with H_2O/Ce >6000, and proposed the presence of a hydrous, deep mantle reservoir
488 formed early in the Earth's history. However, those melts with high Cl/K_2O ≈ 7, Cl/F ≈ 100 and
489 Cl/H_2O ≈ 0.6 ratios were explained by Sobolev et al. (2016) as being due to assimilation of
490 serpentinites altered by seawater with possible involvement of seawater-derived brines. For
491 comparison, Cl/K_2O from 0.23 to 0.65, Cl/F from 2.4 to 3.5, and Cl/H_2O from 0.02 to 0.09 in the
492 studied Gorgona melt inclusions are well below the above values ascribed to contamination by
493 Sobolev et al. (2016), and the controversy remains as to whether the obtained volatile
494 concentrations preserved in the Gorgona melt inclusions are pristine or they were inherited
495 during assimilation of crustal rocks by the magma (e.g., Shimizu et al., 2001; Berry et al., 2008;
496 Kent et al, 2009; Kamenetsky et al., 2010).

497 One of the main arguments against a hydrous origin of the Gorgona komatiites is their
498 extreme depletion in incompatible trace elements. This depletion becomes progressively more
499 pronounced on going from basalts through komatiites to picrites. However, it is clear that all
500 these rock types are related to a similar type of depleted mantle source (e.g., Arndt et al., 1997;
501 Révillon et al., 2000, 2002). These authors ascribed the origin of volatiles (and in particular

502 water) either to sub-solidus alteration processes or to assimilation of hydrated crust in a shallow-
503 level magma reservoir. This latter conclusion was also reached by Shimizu et al. (2009), who in
504 their study of chromites from the beach sands of Gorgona described CO_2-rich (40–4000 µg/g)
505 melt inclusions with highly variable H_2O (0.03–0.9 wt. %) and Cl (6–1056 µg/g) and proposed
506 that the concentrations of volatile components, and especially Cl, were influenced by magma
507 degassing or interaction with seawater or brine prior to entrapment.
508 Significantly, however, Gurenko and Kamenetsky (2011), who studied boron contents
509 and B isotopic compositions in the same melt inclusions analysed during the present study,
510 argued that it was not possible to unequivocally prove magma contamination only on the basis of
511 Cl/K_2O vs. H_2O/K_2O relationships (or similar, where Cl- and H_2O-concentrations are normalised
512 to a concentration of an incompatible element). These authors showed that although H_2O/K_2O-
513 Cl/K_2O or H_2O/K_2O-B/K_2O systematics can be explained by contamination of magma by
514 seawater or NaCl-rich brines, the relationships between B/K_2O and Cl/K_2O or B/K_2O and $\delta^{11}B$,
515 for the same inclusions do not support their role, as well as a role of altered oceanic crust,
516 serpentinites or marine sediments as possible contaminants.
517 The highest obtained $H_2O/Ce = 4490$ of the studied melt inclusions is significantly lower
518 than that of the Archaean komatiites (H_2O/Ce >6000; Sobolev et al., 2016) and the highest
519 $CO_2/Nb = 3320$ and $Zr/Y = 2.1$ are very close to, but $F/Zr = 2.6$ is significantly lower than, those
520 of the "primary komatiite" of Shimizu et al. (2009) (i.e., $CO_2/Nb = 4000 \pm 2200$, $F/Zr = 7.0 \pm$
521 1.7, $Zr/Y = 1.7 \pm 0.3$). In addition to not being as high as in this hypothetical "primary
522 komatiite", the F/Zr ratios (1.5–2.6) in the olivine melt inclusions analysed in this study, are at
523 the lower end of the F/Zr range in the chromite-hosted inclusions of Shimizu et al. (2009). We
524 note that all chromites studied by Shimizu et al. (2009) are from the beach sands and are likely to
525 come from any type of mafic rocks exposed on Gorgona, not necessarily from komatiites. This
526 may suggest that the inclusions analysed during the present study and those of Shimizu et al.

527 (2009) perhaps represent two similar but quite different magmatic systems, at least with respect
528 to their dissolved volatiles.
529 The observed significant correlations of S, and to a lesser extent H_2O, with almost all
530 highly incompatible elements **(Fig. 4b, d)**, the good correlation between F and Cl **(Fig. 4e)**, in
531 addition to there being no clear relationship between Cl and H_2O, suggest that neither shallow
532 magma degassing nor crustal contamination have affected volatile concentrations in the studied
533 magmas during ascent.
534 Moreover, if rapid crystallization of skeletal olivine occurred at shallow crustal depth (no
535 deeper then ~2.5 km, as follows from CO_2-H_2O data) during magma transport to the surface and
536 probably continued *in-situ* in the lava flow, in contrast to the much slower crystallization in a
537 magma chamber, then H_2O (as well as chlorine and probably other volatiles) must have been
538 supplied to the magma by interaction with near-surface, seawater pre-conditioned crustal rocks.
539 This would imply crystallization of olivine with higher than "normal mantle" $\delta^{18}O$ composition
540 (i.e., 4.8–5.4‰), because upper-level crustal rocks suffered low-temperature (<300 ºC) alteration
541 by seawater are characterized by elevated, up to 13‰, $\delta^{18}O$ values (see above). Since the
542 majority of the studied olivines are "mantle"-like in respect of $\delta^{18}O$, we consider the possibility
543 of surface contamination of the komatiite parental magma by variable amount of seawater-
544 preconditioned crustal components as unlikely.
545
546 *5.4. Boron vs. oxygen isotope relationships*
547 Boron vs. oxygen isotope systematics have been shown to be a very powerful tool in
548 discriminating between pure mantle melting and crust recycling, slab-mantle wedge interaction
549 or shallow depth magma contamination. In particular, Chaussidon and Jambon (1994),
550 Chaussidon and Marty (1995), Smith et al. (1995) have demonstrated on primitive MORB and
551 OIB glasses that positive $\delta^{11}B$ associated with increasing oxygen isotope ($\delta^{18}O$ >5.5‰) and

552 radiogenic Sr isotope ratios are more likely to result from shallow-level assimilation of oceanic
553 crust, whereas negative $\delta^{11}B$ values accompanied by low $\delta^{18}O$ <5.5‰ point towards interaction
554 of primitive magmas with the Layer 3 gabbroic crust. Moreover, the systematically higher $\delta^{11}B$,
555 reported for arc lavas by Peacock and Hervig (1999), as compared to exhumed subduction
556 related metamorphic rocks, may suggest that dehydration reactions can significantly decrease
557 $\delta^{11}B$ of the subducting oceanic crust and sediments, thereby implying significant fractionation of
558 ^{11}B and ^{10}B and enrichment of the fluid in ^{11}B isotope.

559 Although variable but generally positive $\delta^{11}B$ values have been identified in mantle
560 wedge serpentinites at the slab-mantle interface (e.g., Benton et al., 2001; Savov et al., 2005,
561 2007), it has also been shown that subduction-related serpentinites, eclogites and slab-derived
562 melts may be strongly depleted in ^{18}O, and have significantly lower $\delta^{18}O$ than that of typical
563 mantle (down to ~2–4‰) (e.g., Bindeman et al., 2005; Bindeman 2008; Martin et al., 2011;
564 Jacques et al., 2013). In addition, Martin et al. (2011) have demonstrated that slab-derived fluids
565 can be markedly enriched in ^{18}O, if dehydration occurred at low T, i.e., <300ºC. This is because
566 the fluid-rock O-isotope fractionation factor, $\Delta^{18}O_{fluid\text{-}rock}$, can be as high as 10‰ at this
567 temperature. But O-isotope composition of the fluid can broadly correspond to the composition
568 of the source rock if released at higher temperatures (because $\Delta^{18}O_{fluid\text{-}rock} \approx 0$ at T >400 ºC).

569 Gurenko and Kamenetsky (2011) previously identified two groups of Gorgona olivine-
570 hosted melt inclusions in B-$\delta^{11}B$ space. The first group of inclusions has relatively low $\delta^{11}B$
571 from −11.5 to −7.3‰ (average −9.0 ± 1.5‰), spanning the entire range of B concentrations and
572 closely corresponding to the Earth's mantle value of −10 ± 2‰ (Chaussidon and Marty, 1995).
573 The second group is characterised by generally higher $\delta^{11}B$ values than mantle $\delta^{11}B$ (up to
574 +15.6‰) and increasing B concentrations up to 1.6 µg/g (see Fig. 3 in Gurenko and
575 Kamenetsky, 2011). The first group was interpreted to be of mantle origin, whereas the second
576 was explained by input of <3 wt.% of ^{11}B-enriched (possibly subduction related) fluid into the

source of the Gorgona komatiites. The main limitation of the proposed mechanism, however, is the absence of a clear geochemical signature of subduction in the composition of the studied melt inclusions such as depletion of high field strength elements (Nb, Zr, Ti) coupled with U-shaped patterns of incompatible element spectra due to the enrichment of large ion lithophile elements (Rb, Ba, K, Sr) and Pb. It is important to note that a similar absence of the subduction signatures in the H_2O-rich olivine-hosted melt inclusions from the 2.7-billion-year-old komatiites from the Abitibi greenstone belt in Canada led Sobolev et al (2016) to propose the presence of a hydrous deep-mantle reservoir in the Archaean mantle.

Figure 6 shows the B isotopic composition of Gorgona melt inclusions from Gurenko and Kamenetsky (2011) linked with new O-isotopic data on the hypothetical melts in equilibrium with olivines, for which $\delta^{18}O_{Ol}$ were determined (olivine equivalent). In order to calculate the O isotope fractionation factor we used a coefficient $A = -0.54$ in the general isotope fractionation equation:

$$\Delta^{18}O_{ol\text{-}melt} = A \times 10^6/T^2 \qquad \text{Eq. 1}$$

defined for komatiite by Matthews et al. (1998). The calculated $\Delta^{18}O_{ol\text{-}melt}$ was found to be between –0.199 and –0.212 in the T-range of 1320–1380 ºC, i.e., the crystallization temperatures of the studied olivines (Kamenetsky et al., 2010). Surprisingly, but even with a large range of boron isotopic composition from −11.5 to 15.6‰ of $\delta^{11}B$, the assigned $\delta^{18}O_{melt}$ values only slightly exceed the "mantle" interval, ranging from 5.0 to 5.9‰, whilst the inclusions of the first, low-$\delta^{11}B$ group of Gurenko and Kamenetsky (2011) fit almost entirely the "mantle" array in respect of both O and B isotope systematics **(Fig. 6)**.

Although the mantle origin of the first, low-$\delta^{11}B$ group of inclusions can be determined on the basis of combined $\delta^{11}B$-$\delta^{18}O$ isotopic data, the origin of the second group of inclusions

602 with varying δ^{11}B data remains enigmatic. We have calculated several two-component mixing
603 trends in δ^{18}O-δ^{11}B space **(Fig. 6)**, illustrating the effects of possible interaction of fluids
604 released from oceanic crust at different temperatures, with a MORB-like depleted mantle source,
605 as well as the effects of the possible presence of recycled crust and variously dehydrated
606 serpentinite in the magma source cf. Gurenko and Kamenetsky (2011). We used B contents and
607 δ^{11}B values of the mixing end-members as defined by Gurenko and Kamenetsky (2011) coupled
608 with the respective oxygen isotope data (for explanation see **Table S2.3** – *Supporting online*
609 *material*). As shown by the calculations, our new B-O isotopic data also confirm the importance
610 of a H_2O- and B-rich fluid component released at low *T* (*FL1*) and/or serpentinite (*SERP1*)
611 interacting with mantle source rocks (less than 5% of input is required) and, in contrast,
612 demonstrate the unlikely, but still possible, role of the recycled crust (*REC*), dehydrated
613 serpentinite (*SERP2*) and fluids released at greater depths and higher temperatures (*FL2* and
614 *FL3*) (more than 10% addition to the source is required). However, we note that although the
615 potential role of each of the selected mixing end-members cannot be completely ruled out taking
616 into account the analytical precision of δ^{11}B and δ^{18}O determinations, their possible admixture to
617 the *MANT* source should not significantly affect the volatile concentrations of the resulting melts
618 as no difference in volatile contents exists between high-δ^{11}B and low-δ^{11}B groups of inclusions.
619 However, the question exists as to whether the Gorgona picrites and komatiites came
620 from a distinct or a compositionally similar mantle source. As noted by Kerr et al. (1996), in
621 addition to the difference in major and trace element ratios (e.g., Al/Ti, Ce/Sm, Gd/Yb), they
622 also show a subtle difference in their radiogenic isotope signatures, suggesting that their mantle
623 source is unlikely to be the same. Similar conclusions also can be derived from the two distinct
624 trends of magma fractionation in the Fo-NiO diagram (**Fig. 2b**). As shown by several recent
625 studies, Ni concentration in olivine (along with Mn and Ca) is a very good proxy to access
626 relative contribution of the peridotite (mantle) and pyroxenite (recycled crust) components in the

627 mantle source of primary magmas, and these relative contributions can be directly related to the
628 radiogenic isotope composition of the host lavas (e.g., Sobolev et al., 2007, 2008; Gurenko et al.,
629 2013, among others). Using the Sobolev et al. (2008) parameterisation for Ni in olivine, we
630 obtain substantially different fractions of anticipated pyroxenite-derived melt in the picritic (X_{pxm}
631 = 0.27 ± 0.07, 1 SD) and "komatiitic" (X_{pxm} = 0.40 ± 0.06, 1 SD) primary melts that also may
632 partially account for the observed subtle difference in oxygen and radiogenic isotope
633 compositions. Further implications of this method for the possible variability in mineral,
634 chemical and isotopic compositions of these types of rocks are beyond the scope of the present
635 paper. However, given that clinopyroxene is a major inventory of H_2O as, for instance, in the
636 depleted, MORB-like mantle (e.g., Danyushevsky et al., 2000), differences in pristine
637 concentrations of H_2O in Gorgona picrite and "komatiite" parental magmas (where komatiites
638 are more H_2O-rich) can be predicted.
639
640 **6. Conclusions**
641 1. The $\delta^{18}O$ values in the studied olivines from one picrite and five komatiites of Gorgona,
642 Colombia, range from 4.7 to 6.0‰, with the majority (~66% population) being within the
643 typical "mantle" olivine range of 4.8–5.4‰, but with a subordinate but still significant
644 number (~33% population) above, and only 2 olivine grains below, this range. No zoning or
645 systematic difference in forsterite contents and $\delta^{18}O_{Ol}$ values between the internal and
646 external parts of the grains have been recognised.
647 2. The probability density distribution curves reveal a common maximum of $\delta^{18}O_{Ol}$ at ~5.3‰ for
648 both internal and external zones of olivine, but the "rims" exhibit also an additional,
649 subordinate maximum at ~5.6‰ probably due to diffusive oxygen isotope exchange between
650 fresh and low-temperature alteration domains in the olivines. The O-isotope mantle signature
651 of the majority of the studied olivines do not support shallow depth contamination of the

Gorgona high-Mg magmas, and rather favour a deep mantle origin of high volatile concentrations in the olivine-hosted melt inclusions.

3. The concentrations of volatile components in olivine-hosted melt inclusions analysed during the present study agree well with our previously reported data. After correction for post-entrapment crystallization of olivine in the inclusions upon cooling, the concentrations of CO_2 and H_2O reveal minimum pressure estimates of 5–30 MPa, which likely indicate the last vapour-melt equilibrium shortly prior to eruption of magma (<1 km crustal depth). However, ~87% and ~2% of the original CO_2 and H_2O, respectively, have been lost to the inclusion shrinkage bubbles during magma cooling. After correction for this effect, the obtained presumable undegassed ranges of volatile concentrations imply a H_2O-CO_2 gas pressure of 86 ± 44 MPa or ~2.5 km of crustal depth of olivine crystallisation.
4. Significant correlations of S and, to a lesser extent of H_2O, with a number of highly incompatible elements, along with the correlation between F and Cl, but no clear relationship of H_2O with Cl, argue against shallow depth degassing and/or crustal contamination of the studied magmas.
5. The new B-O isotopic data confirm the importance of a H_2O- and B-rich fluid component interacting with the source rocks of the Gorgona magmas, but reduce the likelihood of a role for recycled crust and serpentinite. Therefore, the results of this study suggest that the reported enrichment of volatile components and boron represent a deep mantle signature of the studied Gorgona mafic and ultramafic magmas.

Acknowledgments

We thank Olivier Royer (*Service Commun de Microscopie Électronique et de Microanalyses, Université de Lorraine*) for technical assistance during electron microprobe analyses, and Alex Sobolev for fruitful discussions. The insightful reviews of Sally A. Gibson and two anonymous

677 referees helped us to improve the manuscript. Editorial handling of the paper by Michael J.
678 Bickle is gratefully acknowledged. The Museum of Natural History, Washington, DC, kindly
679 provided us with the standards for EPMA. All analytical costs were covered by CRPG (AAG's
680 internal funds). This is CRPG contribution number *24xx*.
681
682

683 **References**

684 Allègre, C.J., 1982. Genesis of Archean komatiites in a wet ultramafic subducted plate. In:
685 Arndt, N., Nisbet, E.G. (Eds.) Komatiites. Berlin, Springer-Verlag, 495–500.

686 Alt, J.C., Muehlenbachs, K., Honnorez, J. 1986. An oxygen isotopic profile through the upper
687 kilometer of the oceanic crust, DSDP Hole 504B. Earth and Planetary Science Letters 80,
688 217–229.

689 Arndt, N.T., Nisbet, E.G., 1982. Komatiites. Fifth Edition, George Allen and Unwin, London,
690 pp. 526.

691 Arndt, N.T., Kerr, A.C., Tarney, J., 1997. Dynamic melting in plume heads: The formation of
692 Gorgona komatiites and basalts. Earth and Planetary Science Letters 146, 289–301.

693 Arndt, N., Ginibre, C., Chauvel, C., Albarède, F., Cheadle, M., Herzberg, C., Jenner, G., Lahaye,
694 Y., 1998. Were komatiites wet? Geology 26, 739–742.

695 Aitken, B.G., Echeverría, L.M., 1984. Petrology and geochemistry of komatiites and tholeiites
696 from Gorgona Island, Colombia. Contributions to Mineralogy and Petrology 86, 94–105.

697 Bebout, G.E., Barton, M.D., 1989. Fluid flow and metasomatism in a subduction zone
698 hydrothermal system: Catalina Schist terrane, California. Geology 17, 976–980.

699 Benton, L.D., Ryan, J.G., Tera, F., 2001. Boron isotope systematics of slab fluids as inferred
700 from a serpentine seamount, Mariana forearc. Earth and Planetary Science Letters 187,
701 273–282.

702 Berry, A.J., Danyushevsky, L.V., O'Neill, H.St.C., Newville, M., Sutton, S.R., 2008. Oxidation
703 state of iron in komatiitic melt inclusions indicates hot Archaean mantle. Nature 455,
704 960–963.

705 Bickle, M.J., Ford, C.E., Nisbet, E.G., 1977. The petrogenesis of peridotitic komatiites: evidence
706 from high-pressure melting experiments. Earth and Planetary Science Letters 37, 97–106.

707 Bindeman, I., 2008. Oxygen isotopes in mantle and crustal magmas as revealed by single crystal
708 analysis. In: Putirka, K.D., Tepley III, F.J. (Eds.) Minerals, Inclusions and Volcanic
709 Processes. Rev. Mineral. Geochem. 69, Mineral. Soc. Am., Washington DC, pp 445–478.

710 Bindeman, I.N., Eiler, J.M., Yogodzinski, G.M., Tatsumi, Y., Stern, C.R., Grove, T.L.,
711 Portnyagin, M., Hoernle, K., Danyushevsky, L.V., 2005. Oxygen isotope evidence for slab

712 melting in modern and ancient subduction zones. Earth and Planetary Science Letters 235,
713 480–496.
714 Bindeman, I.N., Sigmarsson, O., Eiler, J.M., 2006. Time constraints on the origin of large
715 volume basalts derived from O-isotope and trace element mineral zoning and U-series
716 disequilibria in the Laki and Grímsvötn volcanic system. Earth and Planetary Science Letters
717 245, 245–259.
718 Bindeman, I.N., Gurenko, A.A., Sigmarsson, O., Chaussidon, M., 2008. Oxygen isotope
719 heterogeneity and disequilibria of olivine phenocrysts in large volume basalts from Iceland:
720 evidence for magmatic digestion and erosion of Pleistocene hyaloclastites. Geochimica et
721 Cosmochimica Acta 72, 4397–4420.
722 Birner, S.K., Warren, J.M., Cottrell, E., Davis, F.A., 2016. Hydrothermal alteration of seafloor
723 peridotites does not influence oxygen fugacity recorded by spinel oxybarometry. Geology 44,
724 535–538.
725 Campbell, I.H., Griffiths, R.W., Hill, R.I., 1989. Melting in an Archaean mantle plume: heads it's
726 basalts, tails it's komatiites. Nature 339, 697–699.
727 Carroll, M.R., Webster, J.D., 1994. Solubilities of sulfur, noble gases, nitrogen, chlorine, and
728 fluorine in magmas. In: Carroll, M.R., Holloway, J.R. (Eds.) Volatiles in magmas. Rev.
729 Mineral. 30, Mineral. Soc. Am., Washington DC, pp 231–279.
730 Chaussidon, M., Jambon, A., 1994. Boron content and isotopic composition of oceanic basalts:
731 geochemical and cosmochemical implications. Earth and Planetary Science Letters 121,
732 277–291.
733 Chaussidon, M., Marty, B., 1995. Primitive boron isotope composition of the mantle. Science
734 269, 383–386.
735 Chiba, H., Chacko, T., Clayton, R.N., Goldsmith, J.R., 1989. Oxygen isotope fractionations
736 involving diopside, forsterite, magnetite, and calcite: application to geothermometry.
737 Geochimica et Cosmochimica Acta 53, 2985–2995.
738 Clague, D.A., Moore, J.G., Dixon, J.E., Friesen, W.B., 1995. Petrology of submarine lavas from
739 Kilauea's Puna Ridge, Hawaii. Journal of Petrology 36, 299–349.

740 Condomines, M., Grönvold, K., Hooker, P.J., Muehlenbachs, K., O'Nions, R.K., Óskarsson, N.,
741 Oxburgh, E.R., 1983. Helium, oxygen, strontium and neodymium isotopic relationships in
742 Icelandic volcanics. Earth and Planetary Science Letters 66, 125–136.
743 Danyushevsky, L.V., Eggins, S.M., Falloon, T.J., Christie, D.M., 2000. H_2O abundance in
744 depleted to moderately enriched mid-ocean ridge magmas; Part I: Incompatible behaviour,
745 implications for mantle storage, and origin of regional variations. Journal of Petrology 41,
746 1329–1364.
747 Danyushevsky, L.V., McNeill, A.W., Sobolev, A.V., 2002. Experimental and petrological
748 studies of melt inclusions in phenocrysts from mantle-derived magmas: an overview of
749 techniques, advantages and complications. Chemical Geology 183, 5–24.
750 Day, J.M.D., Pearson, D.G., Macpherson, C.G., Lowry, D., Carracedo, J.-C., 2009. Pyroxenite-
751 rich mantle formed by recycled oceanic lithosphere: oxygen-osmium isotope evidence from
752 Canary Island lavas. Geology 37, 555–558.
753 Dietrich, V.J., Gansser, A., Sommerauer, J., Cameron, W.E., 1981. Palaeogene komatiites from
754 Gorgona Island, East Pacific – A primary magma for ocean floor basalts? Geochemical
755 Journal 15, 141–161.
756 Dixon, J.E., Stolper E.M. 1995. An experimental study of water and carbon dioxide solubilities
757 in mid-ocean ridge basaltic liquids. Part II: Applications to degassing. Journal of Petrology
758 36, 1633–1646.
759 Dixon, J.E., Clague, D.A., Wallace, P., Poreda, R., 1997. Volatiles in alkalic basalts from the
760 North Arch Volcanic Field, Hawaii: Extensive degassing of deep submarine-erupted alkalic
761 series lavas. Journal of Petrology 38, 911–939.
762 Echeverría, L.M., 1980. Tertiary or Mesozoic komatiites from Gorgona island, Colombia: field
763 relations and geochemistry. Contributions to Mineralogy and Petrology 73, 253–266.
764 Echeverría, L.M., Aitken, B.G., 1986. Pyroclastic rocks: Another manifestation of ultramafic
765 volcanism on Gorgona Island, Colombia. Contributions to Mineralogy and Petrology 92,
766 428–436.

767 Eiler, J.M., 2001. Oxygen isotope variations in basaltic lavas and upper mantle rocks. In: Valley,
768 J.W., Cole, D.R. (Eds.) Stable Isotope Geochemistry. Rev. Mineral. Geochem. 43, Mineral.
769 Soc. Am., Washington DC, pp 319–364.
770 Eiler, J.M., Farley, K.A., Valley, J.W., Stolper, E.M., Hauri, E.H., Craig, H., 1995. Oxygen
771 isotope evidence against bulk recycled sediment in the mantle sources of Pitcairn Island
772 lavas. Nature 377, 138–141.
773 Eiler, J.M., Farley, K.A., Valley, J.W., Hofmann, A.W., Stolper, E.M., 1996. Oxygen isotope
774 constraints on the sources of Hawaiian volcanism. Earth and Planetary Science Letters 144,
775 453–468.
776 Eiler, J.M., Farley, K.A., Valley, J.W., Hauri, E., Craig, H., Hart, S.R., Stolper, E.M., 1997.
777 Oxygen isotope variations in ocean island basalt phenocrysts. Geochimica et Cosmochimica
778 Acta 61, 2281–2293.
779 Esposito, R., Bodnar, R.J., Danyushevsky, L.V., De Vivo, B., Fedele, L., Hunter, J., Lima, A.,
780 Shimizu, N., 2011. Volatile evolution of magma associated with the Solchiaro eruption in
781 the Phlegrean Volcanic District (Italy). Journal of Petrology 52, 2431–2460.
782 Faure, F., Arndt, N., Libourel, G., 2006. Formation of spinifex texture in komatiites: an
783 experimental study. Journal of Petrology 47, 1591–1610.
784 Gansser, A., 1950. Geological and petrological notes on Gorgona island in relation to north-west
785 S America. Schweizerische Mineralogische und Petrographische Mitteilungen 30, 219–237.
786 Gansser, A., Dietrich, V.J., Cameron, W.E., 1979. Palaeogene komatiites from Gorgona Island.
787 Nature 278, 545–546.
788 Garcia, M.O., Ito E., Eiler, J.M., Pietruszka, A.J., 1998. Crustal contamination of Kilauea
789 volcano magmas revealed by oxygen isotope analyses of glass and olivine from Puu Oo
790 eruption lavas. Journal of Petrology 39, 803–817.
791 Genske, F.S., Beier, C., Haase, K.M., Turner, S.P., Krumm, S., Brandl, P.A. 2013. Oxygen
792 isotopes in the Azores islands: crustal assimilation recorded in olivine. Geology 41, 491-
793 494.
794 Gregory, R.T., Taylor, H.P., 1981. An oxygen isotope profile in a section of Cretaceous oceanic
795 crust, Samail Ophiolite, Oman: evidence for $\delta^{18}O$ buffering of the oceans by deep (>5 km)

seawater-hydrothermal circulation at mid-ocean ridges. Journal of Geophysical Research 86, 2737–2755.

Grove, T.L., Parman, S.W., 2004. Thermal evolution of the Earth as recorded by komatiites. Earth and Planetary Science Letters 219, 173–187.

Gurenko, A.A., Kamenetsky, V.S., 2011. Boron isotopic composition of olivine-hosted melt inclusions from Gorgona komatiites, Colombia: New evidence supporting wet komatiite origin. Earth and Planetary Science Letters 312, 201–212.

Gurenko, A.A., Hoernle, K.A., Hauff, F., Schmincke, H.-U., Han, D., Miura, Y.N., Kaneoka, I., 2006. Major, trace element and Nd-Sr-Pb-O-He-Ar isotope signatures of shield stage lavas from the central and western Canary Islands: Insights into mantle and crustal processes. Chemical Geology 233, 75-112.

Gurenko, A.A., Bindeman, I.N., Chaussidon, M., 2011. Oxygen isotope heterogeneity of the mantle beneath the Canary Islands: insights from olivine phenocrysts. Contributions to Mineralogy and Petrology 162, 349–363.

Gurenko, A.A., Geldmacher, J., Hoernle, K.A., Sobolev, A.V., 2013. A composite, isotopically-depleted peridotite and enriched pyroxenite source for Madeira magmas: Insights from olivine. Lithos 170–171, 224–238.

Harris, C., Smith, H.S., le Roex, A.P., 2000. Oxygen isotope composition of phenocrysts from Tristan da Cunha and Gough Island lavas: variation with fractional crystallization and evidence for assimilation. Contributions to Mineralogy and Petrology 138, 164–175.

Harris, C., Roux, P., Cochrane, R., Martin, L., Duncan, A.R., Marsh, J.S. Roex, A.P., Class, C., 2015. The oxygen isotope composition of Karoo and Etendeka picrites: High $\delta^{18}O$ mantle or crustal contamination? Contributions to Mineralogy and Petrology 170, 1–24.

Hartley, M.E., Maclennan, J., Edmonds, M., Thordarson, T., 2014. Reconstructing the deep CO_2 degassing behaviour of large basaltic fissure eruptions. Earth and Planetary Science Letters 393, 120–131.

Hattori, K., Muehlenbachs, K., 1982. Oxygen isotope ratios of the Icelandic crust. Journal of Geophysical Research 87, 6559–6565.

824 Haughton, D.R., Roeder, P.L., Skinner, B.J., 1974. Solubility of sulfur in mafic magmas.
825 Economic Geology 69, 541–567.
826 Herzberg, C., 1995. Generation of plume magmas through time: an experimental perspective.
827 Chemical Geology 126, 1–16.
828 Herzberg, C., Asimow, P.D., Arndt, N., Niu, Y., Lesher, C.M., Fitton, J.G., Cheadle, M.J.,
829 Saunders, A.D., 2007. Temperatures in ambient mantle and plumes: Constraints from
830 basalts, picrites, and komatiites. Geochemistry Geophysics Geosystems 8,
831 DOI:10.1029/2006GC001390.
832 Jacques, G., Hoernle, K., Gill, J., Hauff, F., Wehrmann, H., Garbe-Schonberg, D., van der
833 Bogaard, P., Bindeman, I., Lara, L.E., 2013. Across-arc geochemical variations in the
834 Southern Volcanic Zone, Chile (34.5 – 38.0 degrees S): Constraints on mantle wedge and
835 slab input compositions. Geochimica et Cosmochimica Acta 123, 218–243.
836 Jambon, A. 1994. Earth degassing and large-scale geochemical cycling of volatile elements. In:
837 Carroll, M.R., Holloway, J.R. (Eds.) Volatiles in Magmas, Rev. Mineral. 30, Mineral. Soc.
838 Am., Washington DC, pp 479–517.
839 Kamenetsky, V.S., Crawford, A.J., Meffre, S. (2001). Factors controlling chemistry of magmatic
840 spinel: An empirical study of associated olivine, Cr-spinel and melt inclusions from
841 primitive rocks. Journal of Petrology 42, 655–671.
842 Kamenetsky, V.S., Gurenko, A.A., Kerr, A.C., 2010. Composition and temperature of komatiite
843 melts from Gorgona Island constrained from olivine-hosted melt inclusions. Geology 38,
844 1003–1006.
845 Kent, A.J.R., Hauri, E., Woodhead, J., Hergt, J.M., 2009. Volatile contents of Belingewe
846 komatiites: Mantle volatile contents and the effects of degassing, Geochimica et
847 Cosmochimica Acta 73, A640.
848 Kerr, A.C., 2005. La Isla de Gorgona, Colombia: A petrological enigma? Lithos 84, 77–101.
849 Kerr, A.C., Arndt, N.T., 2001. A note on the IUGS reclassification of the high-Mg and picritic
850 volcanic rocks. Journal of Petrology 42, 2169–2171.

851 Kerr, A.C., Marriner, G.F., Arndt, N.T., Tarney, J., Nivia, A., Saunders, A.D., Duncan, R.A.,
852 1996. The petrogenesis of Gorgona komatiites, picrites and basalts: new field, petrographic
853 and geochemical constraints. Lithos 37, 245–260.
854 Kyser, T.K., Nisbet, E.G., Cameron, W.E., Gansser, A., Dietrich, V.J., 1987. Stable isotope
855 geochemistry and alteration of Cretaceous komatiitic and associated rocks from Gorgona
856 island, Colombia. Geochemical Journal 21, 253–259.
857 Ludwig, K.R. 2008. User's manual for Isoplot 3.70: A geochronological toolkit for Microsoft
858 Excel. Berkeley Geochronology Center, Special Publication No 4, 77 pp.
859 Martin, E., Bindeman, I. Grove, T.L., 2011. The origin of high-Mg magmas in Mt. Shasta and
860 Medicine Lake volcanoes, Cascade Arc (California): higher and lower than mantle oxygen
861 isotope signatures attributed to current and past subduction. Contributions to Mineralogy
862 and Petrology 162, 945–960.
863 Mathez, E.A., 1976. Sulfur solubility and magmatic sulfides in submarine basalt glasses. Journal
864 of Geophysical Research 81, 4269–4276.
865 Mattey, D., Lowry, D., Macpherson, C., 1994. Oxygen isotope composition of mantle peridotite.
866 Earth and Planetary Science Letters 128, 231–241.
867 Matthews, A., Stolper, E.M., Eiler, J.M., Epstein, S., 1998. Oxygen isotope fractionation among
868 melts minerals and rocks. Mineralogical Magazine 62A, 971–972 (Goldschmidt Conference
869 Extended Abstract).
870 McDonough, W.F., Ireland T.R., 1993. Intraplate origin of komatiites inferred from trace
871 elements in glass inclusions. Nature 365, 432–434.
872 Mironov, N., Portnyagin, M., Botcharnikov, R., Gurenko, A., Hoernle, K., Holtz, F., 2015.
873 Quantification of the CO_2 budget and H_2O–CO_2 systematics in subduction-zone magmas
874 through the experimental hydration of melt inclusions in olivine at high H_2O pressure. Earth
875 and Planetary Science Letters 425, 1–11.
876 Moore, L.R., Gazel, E., Tuohy, R., Lloyd, A.S., Esposito, R., Steele-MacInnis, M., Hauri, E.H.,
877 Wallace, P.J., Plank, T., Bodnar, R.J., 2015. Bubbles matter: An assessment of the
878 contribution of vapor bubbles to melt inclusion volatile budgets. American Mineralogist
879 100, 806–823.

880 Muehlenbachs, K., 1986. Alteration of the oceanic crust and the ^{18}O history of seawater. In:
881 Valley, J.W., Taylor Jr., H.P., O'Neil, J.R. (Eds.) Stable Isotopes in High Temperature
882 Geological Processes. Rev. Mineral, 16, Mineral. Soc. Am., Washington DC, pp 425–444.
883 Muehlenbachs, K., Anderson, A.T., Sigvaldason, G.E., 1974. Low-^{18}O basalt from Iceland.
884 Geochimica et Cosmochimica Acta 38, 577–588.
885 Newman, S., Lowenstern, J.B., 2002. VolatileCalc: a silicate melt-H_2O-CO_2 solution model
886 written in Visual Basic for Excel. Computers and Geosciences 28, 597–604.
887 Parman, S.W., Grove, T.L., 2004. Harzburgite melting with and without H_2O: Experimental data
888 and predictive modeling. Journal of Geophysical Research 109, B02201, doi:
889 02210.01029/02003JB002566.
890 Parman, S.W., Grove, T.L., 2005. Komatiites in the plume debate. In: Foulger, G.R., Natland,
891 J.H., Presnallm, D.C., Anderson, D.L. (Eds.) Plates, Plumes, and Paradigms, GSA Special
892 Publication 388, 249–256.
893 Parman, S.W., Dann, J.C., Grove, T.L., de Wit, M.J., 1997. Emplacement conditions of
894 komatiite magmas from the 3.49 Ga Komati Formation, Barberton Greenstone Belt. South
895 Africa. Earth and Planetary Science Letters 150, 303–324.
896 Peacock, S.M., Hervig, R.L., 1999. Boron isotopic composition of subduction-zone metamorphic
897 rocks. Chemical Geology 160, 281–290.
898 Portnyagin, M., Almeev, R., Matveev, S., Holtz, F., 2008. Experimental evidence for rapid water
899 exchange between melt inclusions in olivine and host magma. Earth and Planetary Science
900 Letters 272, 541–552.
901 Putlitz, B., Matthews, A., Valley, J.W., 2000. Oxygen and hydrogen isotope study of high-
902 pressure metagabbros and metabasalts (Cyclades, Greece): Implications for the subduction
903 of oceanic crust. Contributions to Mineralogy and Petrology 138, 114–126.
904 Révillon, S., Arndt, N.T., Chauvel, C., Hallot, E., 2000. Geochemical study of ultramafic
905 volcanic and plutonic rocks from Gorgona Island, Colombia: The plumbing system of an
906 oceanic plateau. Journal of Petrology 41, 1127–1153.
907 Révillon, S., Chauvel, C., Arndt, N.T., Pik, R., Martineau, F., Fourcade, S., Marty, B., 2002.
908 Heterogeneity of the Caribbean plateau mantle source: Sr, O and He isotopic compositions

of olivine and clinopyroxene from Gorgona Island. Earth and Planetary Science Letters, 91–106.

Savov, I.P., Ryan, J.G, D'Antonio, M., Kelley, K., Mattie, P., 2005. Geochemistry of serpentinized peridotites from the Mariana Forearc – Conical Seamount, ODP Leg 125: Implications for the elemental recycling at subduction zones. Geochemistry Geophysics Geosystems 6, Q04J15, doi:10.1029/2004GC000777.

Savov, I.P., Ryan, J.G., D'Antonio, M., Fryer, P., 2007. Shallow slab fluid release across and along the Mariana arc-basin system: Insights from geochemistry of serpentinized peridotites from the Mariana Forearc. Journal of Geophysical Research 112, B09205, doi:10.1029/2006JB004749.

Serrano, L., Ferrari, L., Martínez, M.L., Petrone, C.M., Jaramillo, C., 2011. An integrative geologic, geochronologic and geochemical study of Gorgona Island, Colombia: Implications for the formation of the Caribbean Large Igneous Province. Earth and Planetary Science Letters 309, 324–336.

Shimizu, K., Komiya, T., Hirose, K., Shimizu, N., Maruyama, S., 2001. Cr-spinel, an excellent micro-container for retaining primitive melts – implications for a hydrous plume origin for komatiites. Earth and Planetary Science Letters 189, 177–188.

Shimizu, K., Shimizu, N., Komiya, K., Suzuki, K., Maruyama, S., Tatsumi, Y., 2009. CO_2-rich komatiitic melt inclusions in Cr-spinels within beach sand from Gorgona Island, Colombia. Earth and Planetary Science Letters 288, 33–43.

Smith, H.J., Spivack, A.J., Staudigel, H., Hart, S.R., 1995. The boron isotope composition of altered oceanic crust. Chemical Geology 126, 119–135.

Sobolev, A.V., Danyushevsky, L.V., 1994. Petrology and geochemistry of boninites from the north termination of the Tonga Trench: constraints on the generation conditions of primary high-Ca boninite magmas. Journal of Petrology 35, 1183–1213.

Sobolev, A.V., Hofmann, A.W., 1999. Incompatible behavior of sulfur in ultra-depleted MORB. Ofioliti 24, 166.

Sobolev, A.V., Hofmann, A.W., Kuzmin, D.V., Yaxley, G.M., Arndt, N.T., Chung, S.-L., Danyushevsky, L.V., Elliott, T., Frey, F.A., Garcia, M.O., Gurenko, A.A., Kamenetsky,

938 V.S., Kerr, A.C., Krivolutskaya, N.A., Matvienkov, V.V., Nikogosian, I.K., Rocholl, A.,
939 Sigurdsson, I.A., Sushchevskaya, N.M., Teklay, M., 2007. The amount of recycled crust in
940 sources of mantle-derived melts. Science 316, 412–417.
941 Sobolev, A.V., Hofmann, A.W., Brügmann, B., Batanova, V.G., Kuzmin, D.V., 2008. A
942 quantitative link between recycling and osmium isotopes. Science 321, 536.
943 Sobolev, A.V., Asafov, E.V., Gurenko, A.A., Arndt, N.T., Batanova, V.G., Portnyagin, M.V.,
944 Garbe-Schönberg, D., Krasheninnikov, S.P., 2016. Komatiites reveal an Archean hydrous
945 deep-mantle reservoir. Nature 531, 628–632, doi 10.1038/nature17152.
946 Stakes, D.S., Taylor, H.P., 1992. The northern Samail ophiolite: an oxygen isotope, microprobe,
947 and field study. Journal of Geophysical Research 97, 7043–7080.
948 Steele-Macinnis, M., Esposito, R., Bodnar, R.J., 2011. Thermodynamic model for the effect of
949 post-entrapment crystallization on the H_2O–CO_2 systematics of vapor-saturated, silicate melt
950 Inclusions. Journal of Petrology 52, 2461–2482.
951 Viljoen M. J. and Viljoen R. P. (1969a) Evidence for the existence of a mobile extrusive
952 peridotitic magma from the Komati Formation of the Onverwacht Group, Upper Mantle
953 Project. Special Publication – Geological Society of South Africa 2, 87-112.
954 Viljoen M. J. and Viljoen R. P. (1969b) The geology and geochemistry of the Lower Ultramafic
955 Unit of the Onverwacht Group and a proposed new class of igneous rocks, Upper Mantle
956 Project. Special Publication – Geological Society of South Africa 2, 55-85.
957 Wallace, P., Carmichael, I.S.E., 1992. Sulfur in basaltic magmas. Geochimica et Cosmochimica
958 Acta 56, 1863–1874.
959 Wallace, P.J., Kamenetsky, V.S. Cervantes, P., 2015. Melt inclusion CO_2 contents, pressures of
960 olivine crystallization, and the problem of shrinkage bubbles. American Mineralogist 100,
961 787–794.
962 Wang, Z., Eiler, J.M., 2008. Insights into the origin of low-$\delta^{18}O$ basaltic magmas in Hawaii
963 revealed from in situ measurements of oxygen isotope compositions of olivines. Earth and
964 Planetary Science Letters 269, 376–386.
965 Widom, E., Farquhar, J., 2003. Oxygen isotope signatures in olivines from Sao Miguel (Azores)
966 basalts: implications for crustal and mantle processes. Chemical Geology 193, 237–255.

967 Woodhead, J.D., Greenwood, P., Harmon, R.S., Stoffers, P., 1993. Oxygen isotope evidence for
968 recycled crust in the source of EM-type ocean island basalts. Nature 362, 809–813.
969 Yamaoka, K., Ishikawa, T., Matsubaya, O., Ishiyama, D., Nagaishi, K., Hiroyasu, Y., Chiba, H.,
970 Kawahata, H., 2012. Boron and oxygen isotope systematics for a complete section of
971 oceanic crustal rocks in the Oman ophiolite. Geochimica et Cosmochimica Acta 84,
972 543–559.
973
974

975 **Figure captions**

976 **Fig. 1.** Simplified geological map of the Gorgona island (modified after Echeverría,1980; Kerr et
977 al., 1996; Révillon et al., 2000). Sampling locations are marked by sample numbers referred to in
978 the text.

979

980 **Fig. 2.** Elemental and oxygen isotopic composition of olivine from Gorgona picrite and
981 komatiite samples. Panels (A) and (D) represent inter- and intra-sample variations of forsterite
982 contents and $\delta^{18}O_{Ol}$ values, respectively. Shown here *error bars* represent the largest $\pm 2\sigma$
983 analytical uncertainty attained during replicate measurements of the San Carlos olivine standard
984 by EPMA (±0.2 mol.% Fo) and SIMS (±0.4‰ of $\delta^{18}O$). Panels (B) and (C) are variation
985 diagrams of NiO (B) and $\delta^{18}O_{Ol}$ (C) vs. Fo in the central parts and near the grain boundaries; (E)
986 cumulative probability density curves of $\delta^{18}O_{Ol}$ in *Ol core* and *Ol rim* parts calculated using
987 *Isoplot 3.70* (Ludwig, 2008). The *Gorgona Ol literature data* set (panel B) shows Fo and NiO
988 concentrations of olivines from Kamenetsky et al. (2010), Gurenko and Kamenetsky (2011), as
989 well as authors' unpublished data. The *shaded band* (panels C, D, E) denotes the range of typical
990 upper mantle olivine (4.8–5.4‰; Mattey et al. 1994) and of olivine in equilibrium with N-
991 MORB magmas (assuming olivine-melt fractionation of −0.4‰ and the N-MORB range of
992 5.2–5.8‰, Eiler, 2001). Dashed, numbered curves in panel (C) represent the Azores (1) and
993 Hawaii (2) *contamination trends* after Wang and Eiler (2008) and Genske et al. (2013),
994 respectively.

995

996 **Fig. 3.** Concentrations of CO_2 and H_2O dissolved in the olivine-hosted melt inclusions from
997 Gorgona komatiites measured by SIMS before correction for the loss in the shrinkage bubble of
998 CO_2 and H_2O (A) and after the correction applied (B) (see text). Isobars of melt compositions in
999 equilibrium with CO_2-H_2O fluid (*solid lines*) and isopleths of fluid composition (dashed lines

1000 with labels returning molecular fraction of H_2O in the fluid) were calculated using *VolatileCalc*
1001 solution model (Newman and Lowenstern, 2002). Both isoplets and isobars were calculated for a
1002 magma having 47 wt.% SiO_2 at 1360°C, corresponding to the averaged values of the studied
1003 melt inclusions (Kamenetsky et al., 2010). *Error bars* represent average $\pm 2\sigma$ analytical
1004 uncertainty attained within three analytical sessions, i.e., ±14% relative for CO_2 and ±12%
1005 relative for H_2O, and they are smaller than the size of the symbol, if not shown. The data from
1006 Shimizu et al. (2009) are shown for comparison.
1007
1008 **Fig. 4.** Relationships between concentrations of S, H_2O, Cl and F with FeO, SiO_2, Ce and Y in
1009 melt inclusions. (a) FeO vs. S variations. The *MORB & OIB* field presents S concentrations in
1010 presumably undegassed MORB and Hawaiian submarine tholeiitic and alkali basaltic glasses
1011 after Mathez (1976), Clague et al. (1995), Dixon et al. (1997) and Wallace and Carmichael
1012 (1992). Dashed curve represents sulfur solubility in basaltic melts based on the sulfide-saturated
1013 experiments of Haughton et al. (1974). (b) Ce vs. S, (c) SiO_2 vs. H_2O, (d) Y vs. H_2O and (e) F vs.
1014 Cl variations. The observed relationships do not support shallow depth contamination of the
1015 Gorgona high-Mg magmas, and rather favour a deep mantle origin of high volatile
1016 concentrations in the olivine-hosted melt inclusions, in agreement with Kamenetsky et al. (2010),
1017 Gurenko and Kamenetsky (2011) and Sobolev et al. (2016). The positive SiO_2-H_2O correlation
1018 may also be interpreted as reflecting gradually increasing degree of source melting at hydrous
1019 conditions.
1020
1021 **Fig. 5.** Averaged, single-grain oxygen isotope compositions of the studied Gorgona olivines. (A)
1022 $\delta^{18}O_{Ol}$ vs. Fo variation diagram, (B) probability density distribution curves of $\delta^{18}O_{Ol}$ values for
1023 olivine from komatiites and picrite GOR94-32.
1024

Fig. 6. Oxygen versus boron isotopic compositions of olivine hosted melt inclusions from Gorgona komatiites. Subdivision of the inclusions on to "low-δ^{11}B" and "high-δ^{11}B" groups and their respective boron isotopic compositions are from Gurenko and Kamenetsky (2011). To infer oxygen isotope composition of the included melts, we used experimental data of Matthews et al. (1998) for komatiite to calculate O isotope fractionation factor between olivine and melt for the temperature range of 1320–1380 ºC. Two-component mixing lines between the depleted MORB-type mantle (*MANT*), recycled crust (*REC*), serpentinised peridotite (*SERP1* and *SERP2*) and hypothetical oceanic crust fluids released at different temperatures (*FL1*, *FL2* and *FL3*) are shown (for end-member compositions see **Table S2.3**, *Supporting online material*). *Shaded grey field* represents the composition of the mantle, with δ^{11}B of −10 ± 2‰ (Gurenko and Kamenetsky, 2011 and references therein) and δ^{18}O of 5.5 ± 0.5‰, assuming a calculated oxygen isotope fractionation of −0.2‰ between olivine and high-Mg melt and the olivine range of 4.8–5.8‰, as defined in **Fig. 2**.

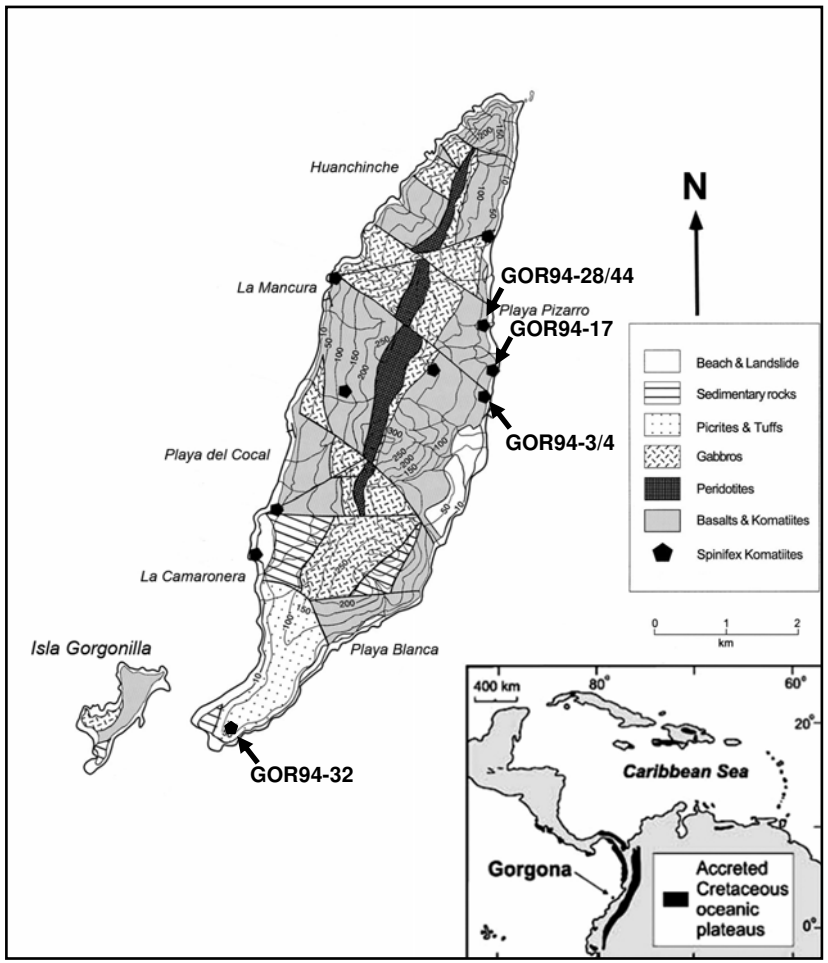

Fig. 1. Gurenko et al.

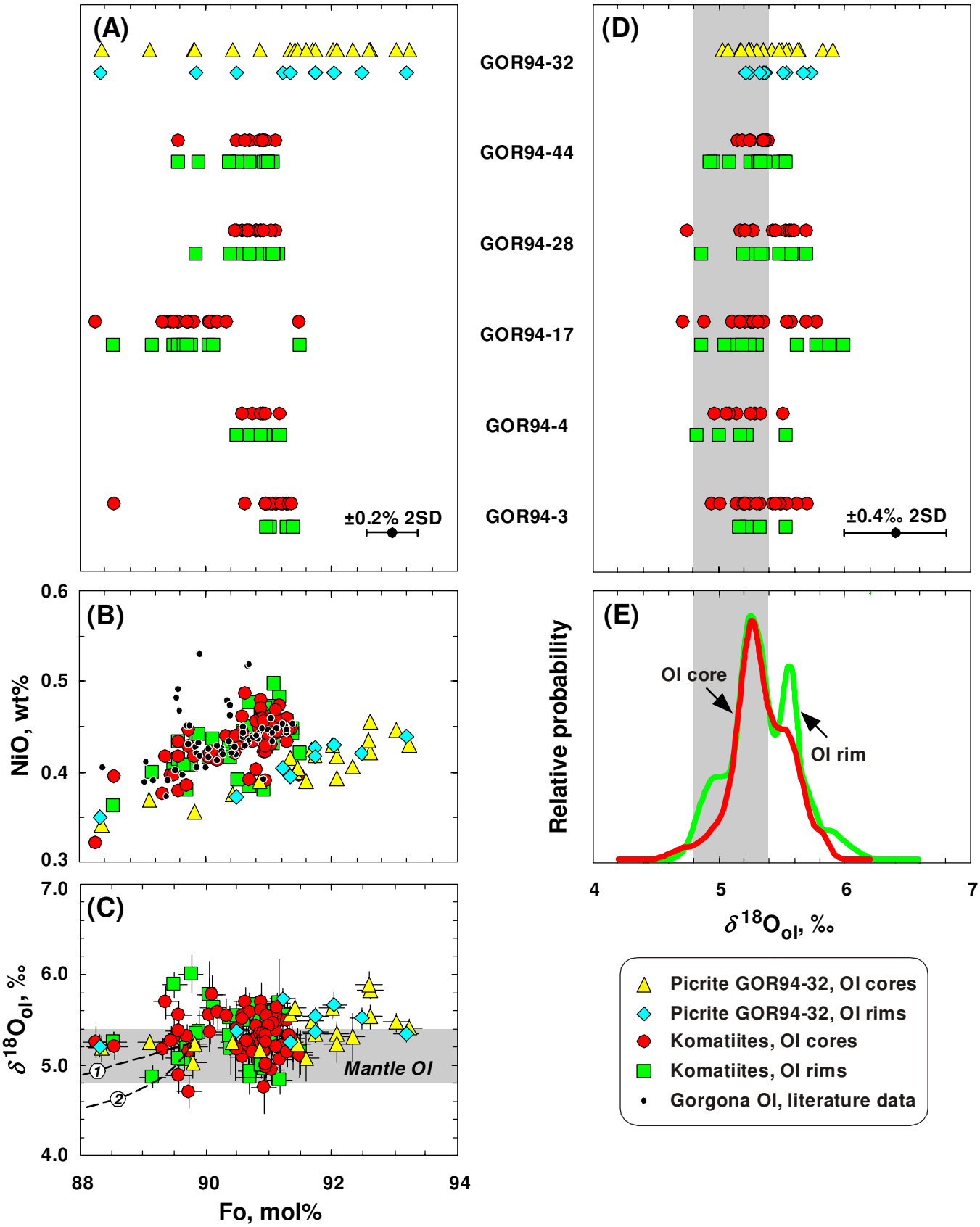

Fig. 2. Gurenko et al.

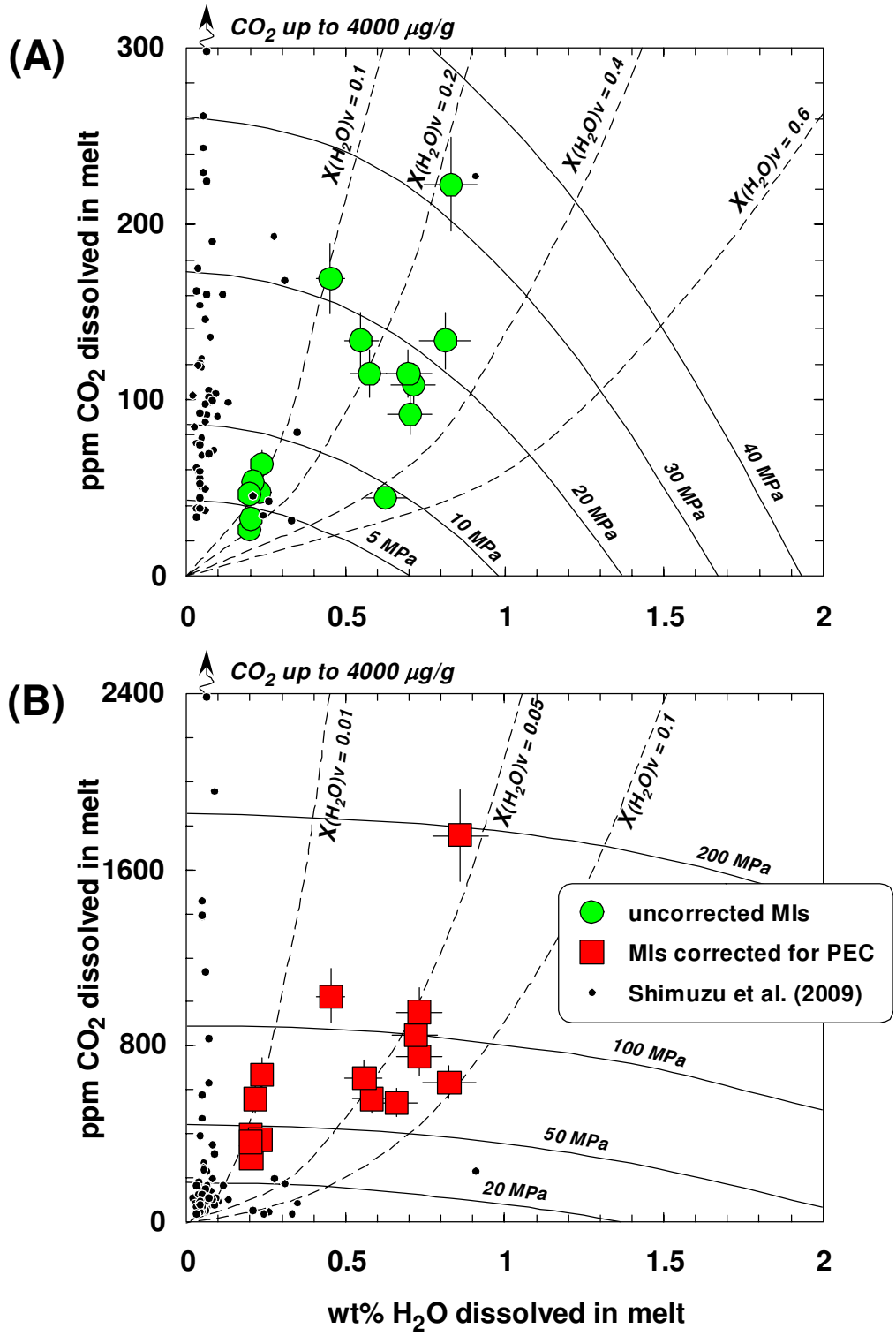

Fig. 3. Gurenko et al.

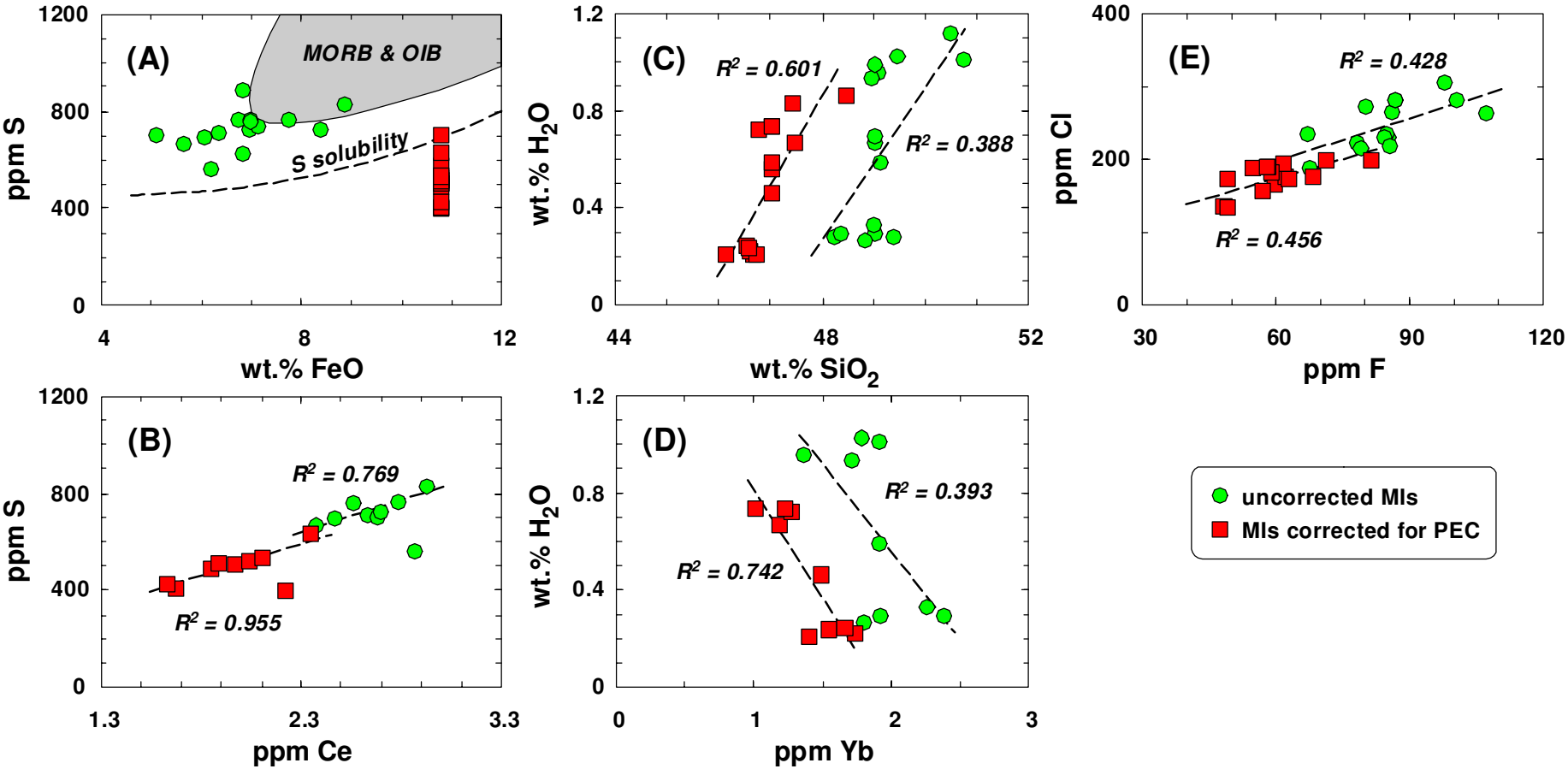

Fig. 4. Gurenko et al.

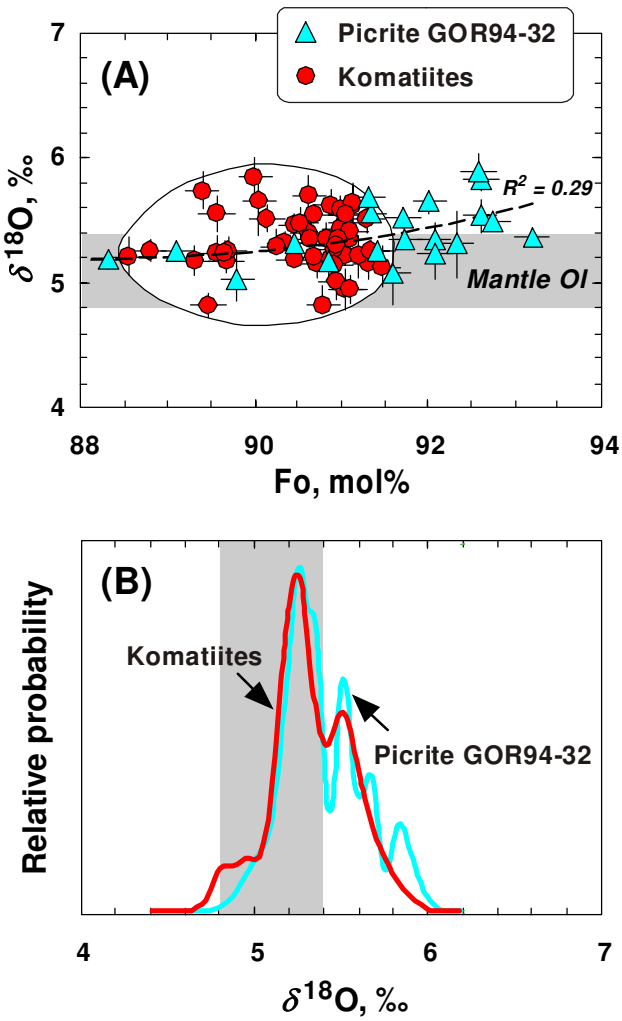

Fig. 5. Gurenko et al.

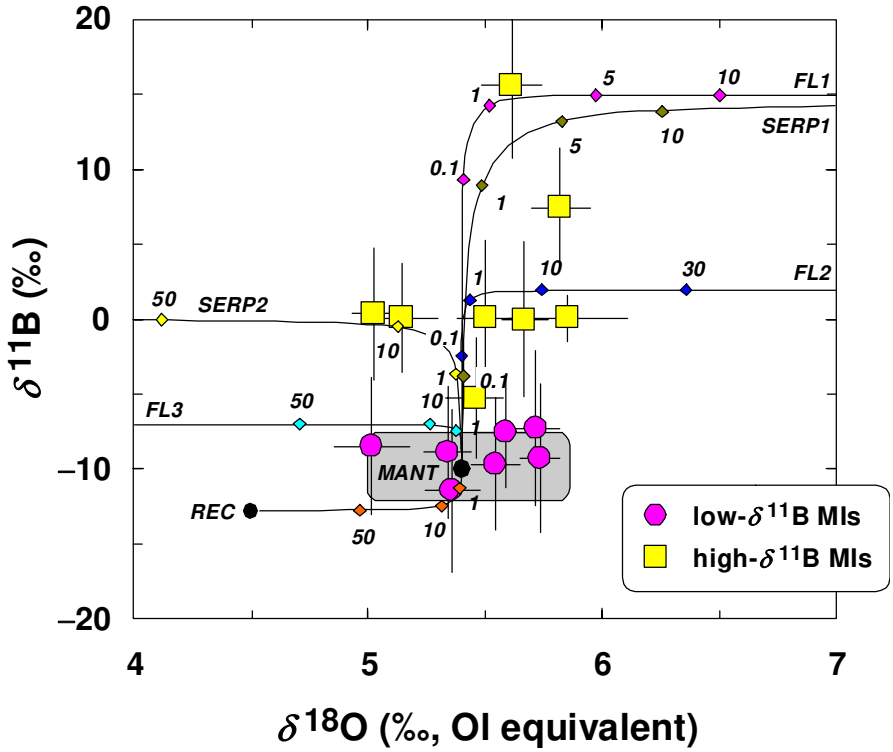

Fig. 6. Gurenko et al.

Supplementary material for online publication only

Click here to download Supplementary material for online publication only: GOR d18O-Ol SOM 4.1.pdf